NTNU

Norwegian University of
Science and Technology

Investigation of WAG Potential using Compositional Model

Tor Hexeberg

Petroleum Geoscience and Engineering
Submission date: June 2016
Supervisor: Jon Kleppe, IPT

Norwegian University of Science and Technology
Department of Petroleum Engineering and Applied Geophysics

Abstract

Water-alternating-gas (WAG) injection is a commonly used enhanced oil recovery (EOR) technique, for which the aim is to increase vertical sweep efficiency and reduce mobility of injected fluids by injecting water and gas in cycles. A company, present on the Norwegian continental shelf, is about to initiate a larger study on the potential of WAG injection for one of its operating fields. This paper serves as an introduction to this study. Some of the benefits and potentially problematic issues during WAG injection have been investigated. Simulation results are used to illustrate and confirm what is found in the literature. For this purpose, the author has created a simplified model of the region in the field model, where WAG injection is planned. This makes it possible to look at WAG effects with a less time-consuming simulation model, before running the field scale model provided by the operating company.

Relative permeability hysteresis due to gas trapping, compositional effects during WAG, effects of high permeable top layer, as well as reservoir management in order to maintain the gas-oil-ratio (GOR) at a reasonable level have been investigated through simulation results.

Sammendrag

Vann-alternerende-gass injeksjon er en vanlig teknikk for å øke oljeutvinningen, der målet er å øke vertikal forskyvningseffektivitet og redusere mobiliteten til de injiserte fluidene ved å injisere vann og gass i sykluser. Et selskap, med tilstedeværelse på den norske kontinentalsokkelen, skal starte en større studie om vann-alternerende-gass injeksjons potensial i et av deres opererende felt. Denne rapporten er ment som en introduksjon til denne studien. Noen av fordelene og potensielle problemstillinger forbundet med vann-alternerende-gass injeksjon har blitt undersøkt. Simuleringsresultater blir brukt til å illustrere og bekrefte det som er funnet i litteraturen. Til dette formålet har forfatteren har laget en forenklet modell av regionen i feltmodellen der vann-alternerende-gass injeksjon er planlagt. Dette gjør det mulig å se på effekter med en mindre tidskrevende modell før man tester ut på feltmodellen som er gjort tilgjengelig av selskapet.

Relativ permeabilitets hysterese grunnet fanget gass, komposisjonelle effekter forbundet med vann-alternerende-gass injeksjon, effekt av høypermeabelt topplag, og reservoarstyring i forhold til å bevare gas-olje forholdet på et rimelig nivå har blitt undersøkt gjennom simuleringsresultater.

Acknowledgement

I would like to thank Lundin Norway AS for providing me with data. I hope that this paper proves useful as an introduction to the larger WAG injection study. I would especially thank Geir Magnus Sæternes. He has provided useful insight and guided me towards the completion of this paper.

Table of Content

List of Figures

List of Tables

Nomenclature

Symbol	Description	SI Unit
Q	Flowrate	m^3/s
A	Area	m^2
k	Permeability	m^2
μ	Viscosity	Pa·s
$\Delta P/\Delta x$	Pressure differential with respect to distance	Pa/m
P	Pressure	Pa
S	Saturation	-
λ	Mobility	-
M	End-point mobility ratio	-
C	Land's trapping coefficient	-

Subscripts

a	Absolute
e	Effective
r	Relative
o	Oil
w	Water
g	Gas
c	Capillary
n	Phase n
adv	Advancing fluid
rec	Receding fluid
norm	Normalized
t	Trapped
c	Critical

Superscript

hy	Hysteresis
i	Imbibition
d	Drainage

1 Introduction

Water alternating gas (WAG) is a long known enhanced oil recovery (EOR) technique. The first reported intentional WAG injection process was conducted in 1957 in Canada. During the following years, up until present day, this EOR technique has been tested in numerous fields with mostly successful results (Christensen, Stenby, & Skauge, 1998).

During a WAG process, water and gas are injected in cycles. A three-phase zone is created when water and gas are injected from the same injection well. The benefit of the three-phase zone is the decreased mobility of the gas and water phases, primarily due to reduced relative permeability, which is highly dependent on trapping of the non-wetting phase. The added mobility control is especially important for the gas phase due to its low viscosity. Reduced mobility of the injected phases increases its displacement efficiency, due to less bypassing behavior.

Gas is usually the most non-wetting phase in a three-phase system. As a result of this, it pushes oil out of the larger pores. When the oil connectivity increases due to higher concentration, water can more easily displace the oil. (Suicmez, Piri, & Blunt, 2006)

The three-phase zone has a limited extension due to gravity effects. Gas moves to the top, while water falls to the bottom. The preference of gas to be on top means that it will sweep oil that water is not able to reach. Down-dip WAG injection and superstructures in the region of WAG injection are examples where this effect would be of special importance (Choudhary et al., 2011).

While WAG injection has many favorable traits, there are also various aspects to be aware of before initiation of this strategy. High permeable zones in the top section of the reservoir would likely create a preferred path for the gas, thus causing early breakthrough and decreasing its spatial extent. These layers, commonly called thief zones caused problems in the Brage field during WAG injection (Lien, Lie, Fjellbirkeland, & Larsen, 1998).

Another issue with WAG injection is the possibility of decreased injectivity of water after injection of gas. This is the downside of the reduced mobility due to the presence of three-phases. If the injection of water from WAG wells is important in order to maintain the pressure in the reservoir, this possible limitation might be a critical factor (Lien et al., 1998), (Kamath, Nakagawa, Boyer, & Edwards, 1998)

1.1 Objective

This paper is supposed to serve as an introduction to a larger WAG study by a company present on the Norwegian shelf. WAG injection is under consideration as a long-term drainage strategy of one of its operating fields.

The paper address some of the important factors of WAG injection found in the literature, such as; uncertainty in relative permeability due to hysteresis and accuracy of models, possible reduction in water injectivity, effect of thief zones, and compositional effects.

Simulation results from a simplified model, with fluid model and other properties provided from the company will be shown in order to better illustrate the WAG effects. Results from a field scale simulation will give some indication of the feasibility of a potential WAG injection strategy.

2 Theory

2.1 Fluid Flow

Understanding the physics related to flow of oil, gas and water is of major importance in the petroleum industry. While the production engineer main issue is with fluid flow through pipes, the reservoir engineers' main concern is with fluid flow through porous medium.

Henry Darcy first described the relationship of fluid flowing through porous medium in Eq. (1.1), popularly called Darcy's law. The original equation was derived for single-phase, one-dimensional flow. Section 2.1.2 will explain how it can be applied to multi-phase systems.

$$Q = -A\frac{k_a}{\mu}\frac{\Delta P}{\Delta x} \tag{1.1}$$

2.1.1 Permeability

Permeability of a porous medium (e.g. reservoir rock) is the area of open pore space perpendicular to the flow direction that is subject to flow (Nolen-Hoeksema, 2014). Absolute permeability is determined when a medium is subject to single-phase fluid flow. Klinkenberg proved, within experimental error, that absolute permeability is generally independent of fluid type as long as the medium is 100 percent saturated with this fluid. The exception to this is gas at low pressures or at very high rates, known as the Klinkenberg effect (Klinkenberg, 1941) (Dake, 1998).

2.1.2 Multi-Phase Systems

Darcy's law assumes single-phase flow. This is rarely valid for flow in a petroleum reservoir in the regions of interest to a reservoir engineer. In an undersaturated oil reservoir (no free gas), connate water is generally still present in the oil zone, making it a two-phase system. As the pressure, in an initially undersaturated oil reservoir, declines below the bubble point, gas is introduced, creating a three-phase system. Only the aquifer would properly satisfy the single-phase assumption.

Since multi-phase flow includes two or more fluids flowing simultaneous, Eq. (1.1) needs to be modified in order to account for the additional complexity. Each phase can be represented by a version of Eq. (1.1), where the absolute permeability is replaced with the effective permeability of the respective phase. The pressure and viscosity are considered for the respective phase. Eq. (1.2) and Eq. (1.3) represent the flow of oil and water in an oil-water system (Dake, 2001). It is important to note that due to interfacial effects between the fluids, the sum of the effective permeabilities will always be less than the absolute permeability (Dake, 1998). The difference between the fluid pressures, called the capillary pressure, is conventionally described as in Eq. (1.4).

$$q_o = A\frac{k_{e,o}}{\mu_o}\frac{\Delta P_o}{\Delta x} \tag{1.2}$$

$$q_w = A\frac{k_{e,w}}{\mu_w}\frac{\Delta P_w}{\Delta x} \tag{1.3}$$

$$P_c = P_{non-wetting} - P_{wetting} \tag{1.4}$$

2.1.3 Relative Permeability

In order to simplify the discussion around effective permeability, a normalized version referred to as relative permeability is usually preferred. This is a dimensionless function ranging between 0 and 1. Eq. (1.5) describes the relationship between relative, effective and absolute permeability for phase n as a function of water saturation in a two-phase system.

$$k_{r,n}(s_w) = \frac{k_{e,n}(s_w)}{k_a} \tag{1.5}$$

It is obvious that relative permeability depends on the saturation or the fluids. However, evidence suggest that relative permeability does not depend solely on saturation, but a range of other parameters such as wettability, pore shape and pore throat (Oren, Bakke, & Arntzen, 1998). Most importantly for this paper is the dependency on the saturation history (Fatemi & Sohrabi, 2012).

2.1.4 Three-Phase Relative Permeability Models

The common approach when estimating three-phase relative permeability is to use an interpolation model in combination with two-phase relative permeability lab data. Two sets of two-phase data must be used and the most common is to use oil-water and oil-gas. The reason for this approach is that it is expensive to produce reliable three-phase relative permeability lab data.

Stone I, Stone II and Cheshire (default in eclipse) are the industry standard three-phase relative permeability models. These models in combination with hysteresis models provide different results. The cyclic nature of saturation changes during WAG injection makes the differences very notable (Kossack, 2000).

According to (Spiteri & Juanes, 2004) Stone I is the model that best correspond to experimental data.

2.1.5 Mobility

Equation (1.6) defines mobility of any fluid. The mobility of a fluid is its capability to flow. This is apparent when comparing it with eq. (1.2) or (1.3), which reveals that mobility is proportional to velocity (Dake, 1998).

$$\lambda = \frac{k_a k_r}{\mu} \tag{1.6}$$

During the process in which one fluid displaces another, the mobility ratio between the two fluids becomes important. End point mobility ratio (M) as defined in (Dake, 1998) is shown in Eq. (1.7). For M > 1 the displacing fluid is capable of flowing faster than the displaced fluid. This implies that the displacing fluid can bypass the displaced fluid creating a fingering displacement. For gas injected into oil the mobility ratio will likely be unfavorable (M > 1) due to low gas viscosity. During WAG injection, the water acts as a mobility control for the gas because it reduces the end-point relative permeability because there are three phases instead of two.

$$M = \frac{\text{Mobility of advancing fluid}}{\text{Mobility of receding fluid}} = \frac{\lambda_{adv}}{\lambda_{rec}} = \frac{k_{r,adv} \big/ \mu_{adv}}{k_{r,rec} \big/ \mu_{rec}} \tag{1.7}$$

2.1.6 Wettability

Wettability is the reservoir rock's preference to one fluid rather than the other fluid(s) present in a sytem. This property affects a fluids ability to flow. (Nolen-Hoeksema, 2014). In a strongly water wet medium, the water will be located on the walls of the pore, and oil in the middle. As long as the water saturation is sufficiently low, the oil can flow though the pore opening. However, if the water saturation increases such that the water closes the pore opening, then the oil become trapped, thus loses its ability to flow. The situation is reverse for a strongly oil-wet reservoir. This type of displacement is called snap-off displacement and is not ideal when high oil recovery by water injection is preferred.

2.1.7 Drainage and Imbibition

Drainage refers to as the process in which the non-wetting fluid displaces the wetting fluid, while imbibition refers to the reverse process. Depending on the wettability of the rock, the wetting fluid could be either water or oil (Suicmez et al., 2006). Gas is usually considered the non-wetting phase, especially in water-wet reservoirs, but can be the intermediate wetting fluid in strongly oil-wet reservoirs. (Suicmez et al., 2006)

Air-water drainage experiments where CT images where obtained post process show how intermediate to large pores have low water saturation and smaller pores have high water saturation. Thus, implying that the wetting phase saturation depends highly on the pore size. Imbibition experiments show that the trapped gas phase is concentrated in the larger pores. (Kumar et al., 2009)

2.1.8 Hysteresis

Hysteresis in multiphase flow can be observed in the relative permeability and capillary pressures due to the dependency on saturation history. **Fig. 2-1** show how the relative permeability depends on the saturation path. The special case where hysteresis is defined at the end-points, arise due to drainage and imbibition from residual saturations. For continuous water injection of an undersaturated oil reservoir, this might be a satisfactory representation of the relative permeability since the oil saturation decreases monotonously as water is injected.

In the case of WAG injection, however, this representation is no longer satisfactory because of the cyclic injection. Cyclic injection lead to cyclic changes in the saturation, generally before the end-points are reached. This means that a representation of relative permeability must be able to predict the new saturation path from the saturation, at which the current drainage/imbibition process is reversed. To represent this with input curves from lab experiments would be impractical, as many curves would be needed in order to give an accurate representation. Models have been created in order to account for the hysteresis (Christensen, Larsen, & Nicolaisen, 2000).

On pore scale there are at least two reasons for hysteresis: **1)** difference in contact angle between the displaced and displacing fluid; **2)** trapping of the non-wetting fluid (Spiteri & Juanes, 2004).

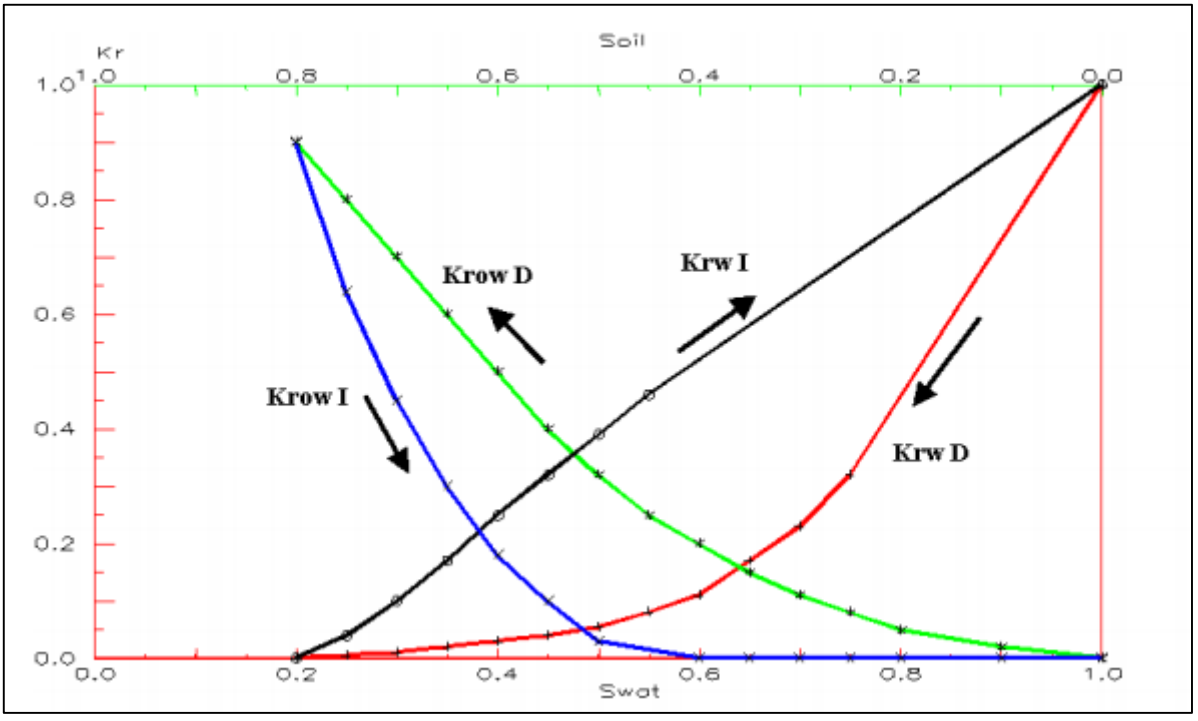

Fig. 2-1 *- Two phase hysteresis in water-wet reservoir (Kossack, 2000). The relative permeability of the fluid phase depends on whether it is the displacing fluid or being displaced. The notation D and I stands for drainage and imbibition respectively.*

2.1.8.1 Gas Trapping

During a drainage-imbibition cycle in water-gas system (Kumar et al., 2009) and oil-gas system (Spiteri & Juanes, 2004), it has been observed that residual gas is trapped in the pores. This observation is described in (Land, 1968) where Eq. (1.8) and (1.9) was proposed to describe the trapped gas saturation.

$$S_{g,t} = \frac{S_g^{hy}}{1 + C + S_g^{hy}} \tag{1.8}$$

$$C = \frac{1}{S_{gt,\max} - S_{gc}} - \frac{1}{S_{g,\max} - S_{gc}} \tag{1.9}$$

Fig. 2-2 illustrates the phenomenon where gas is trapped after a drainage-imbibition cycle in an oil-gas-connate water experiment. This gas trapping behavior is of great importance during a WAG injection because of cyclic drainage and imbibition.

The behavior can be generalized as trapping of the non-wetting phase. This means that in an oil-water system for a water-wet rock, oil will be trapped phase.

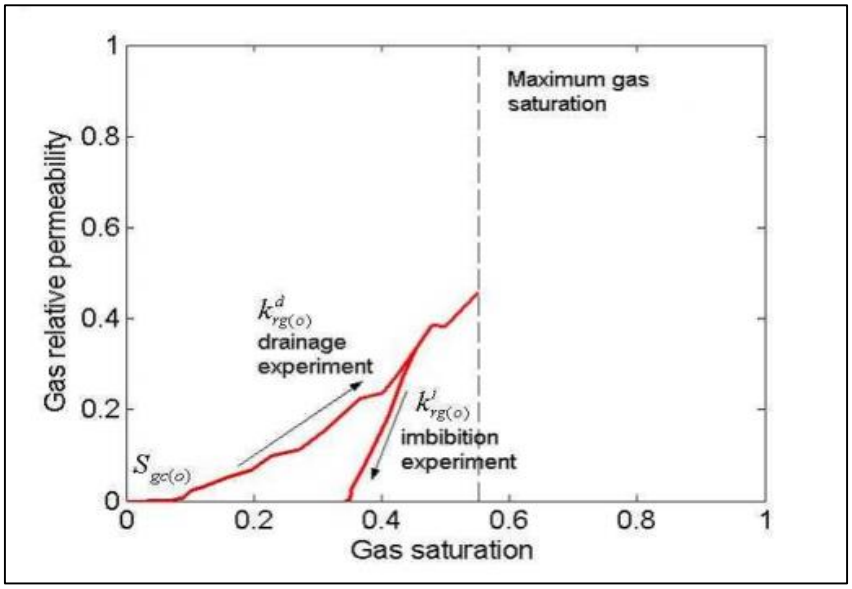

***Fig. 2-2** – Drainage-imbibition cycle in oil-gas-connate water experiment. At the end of the imbibition, where gas is no longer mobile, residual gas still resides in the pores. (Spiteri & Juanes, 2004).*

(Spiteri & Juanes, 2004) conducted different imbibition experiments where absolute permeability and fluid system were variables. **Fig. 2-3** show the calculated Land trapping coefficient (Eq. (1.9)). A low value of Land's coefficient implies high trapping saturation of the non-wetting phase. During a WAG injection, we are mostly concerned with the water-gas and water-oil displacements as these dominate the process. Observe that higher absolute permeability suggest lower trapping of oil, which then will result in higher recovery. The trapping coefficient for the water-gas system are lower than for the water-oil system indicating that gas trapping is the most dominant force and that gas will likely displace the initially trapped oil form the water injection.

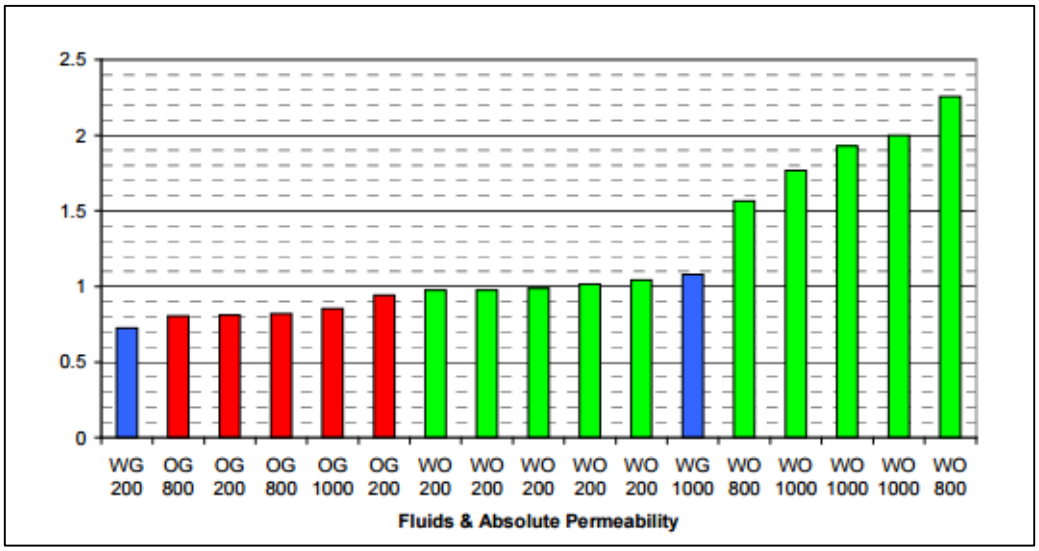

Fig. 2-3 *– Land trapping coefficient for different permeabilities and fluid systems (Spiteri & Juanes, 2004).*

Increased trapping of gas implies an increase in the oil connectivity because oil is squeezed out of the larger pores into smaller pores. This further results in increased oil recovery during the water flooding. This effect can be seen in **Fig. 2-4**, where a low value of the Land parameter equals high degree of trapping.

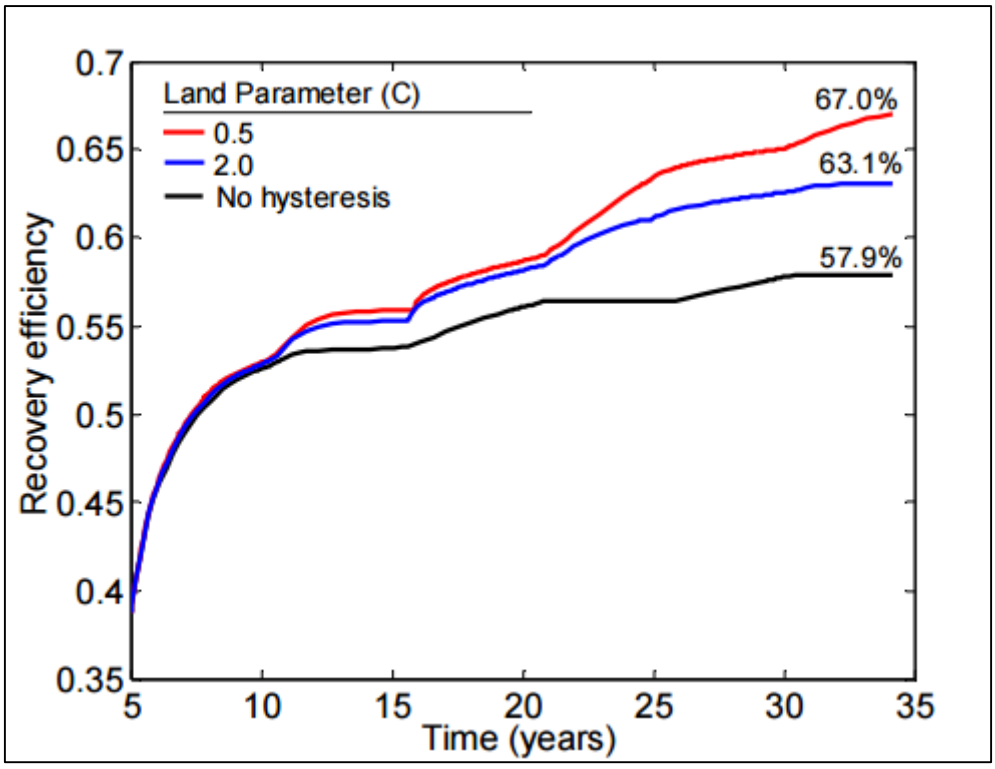

Fig. 2-4 *– Recovery efficiencies using different trapping coefficients during a WAG simulation. The lower value implies more trapping of gas, which in turn give higher oil recovery. WAG three-phase hysteresis model is used (Spiteri & Juanes, 2004).*

2.1.8.2 Hysteresis Models

Two hysteresis models that are commonly used in the industry and implemented in most commercial simulations are; (Killough, 1976) given in Eq.(1.10) and (1.11), and (Carlson, 1981), which is calculated by a stepwise algorithm. The method can be found in the original paper.

$$k_{rg}^{i}(S_g) = \frac{k_{rg(o)}^{i}(S_{g,norm}) \cdot k_{rg(o)}^{d}(S_{g,hy})}{k_{rg(o)}^{d}(S_{g,\max})} \tag{1.10}$$

$$S_{g,norm} = S_{g(o)}^{i} + \frac{(S_g - S_{gt,\max})(S_{g,\max} - S_{g(o)}^{i})}{S_{g,hy} - S_{gt,\max}} \tag{1.11}$$

Both models are based on Land's trapping model in order to create imbibition scanning curves, which are curves that lie between the drainage and imbibition curves, see **Fig. 2-5**. Carlson's model uses the entire imbibition curve to calculate the scanning curve, thus the scanning curve is assumed parallel to the primary imbibition curve. Both models imply that the imbibition scanning curves are reversible for the subsequent drainage.

The two models are created based on two-phase systems, for which the assumption of reversibility of the scanning curve might be acceptable. For three-phase flow, however, the changes in saturations can cause subsequent drainage to differ from the imbibition scanning curve. In application to WAG, gas relative permeability is reduced with increased water saturation. Also water relative permeability is reduced in presence of trapped gas. (Spiteri & Juanes, 2004).

A hysteresis model specifically developed for WAG injection was developed by (Larsen & Skauge, 1998). This model is based on (Carlson, 1981) and (Land, 1968). It accounts for all three phases, and it includes the decreasing pattern of the gas relative permeability with each cycle (Kossack, 2000). In addition to specifying Land's trapping parameter, a secondary drainage reduction parameter can be specified. Imbibition curve for the oil-gas relative permeability is not necessary for the model as it calculates this from the drainage curve.

Fig. 2-6 illustrate the importance of accounting for reduction in gas relative permeability. The simulation is done with an even ratio WAG cycle of ten years starting with five years of water injection. All hysteresis models provide approximately the same results for the second water injection, where trapped gas increases the waters ability to sweep oil. During the second gas cycle, however, the reduction in gas relative permeability in the three-phase model results in lower mobility of the gas, thus better sweep efficiency (Spiteri & Juanes, 2004).

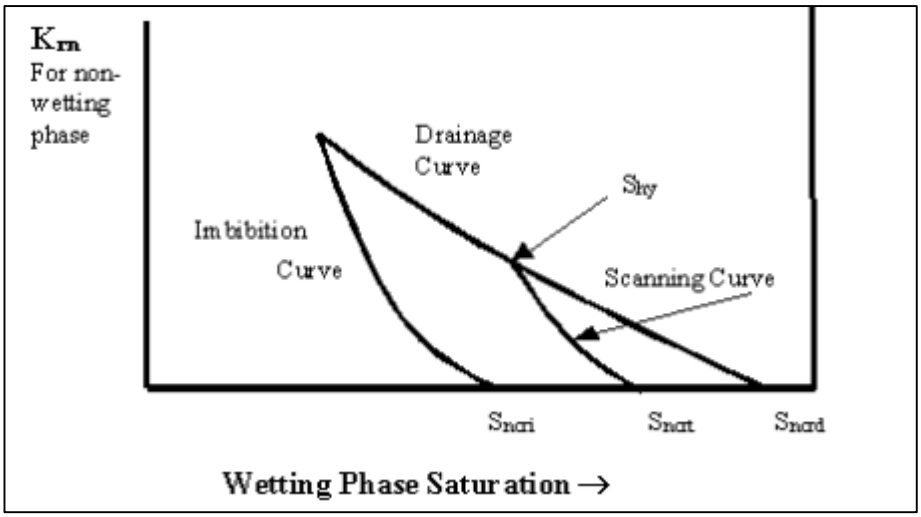

Fig. 2-5 *– Illustration of relative permeability hysteresis using Carlson's model (Kossack, 2000)*

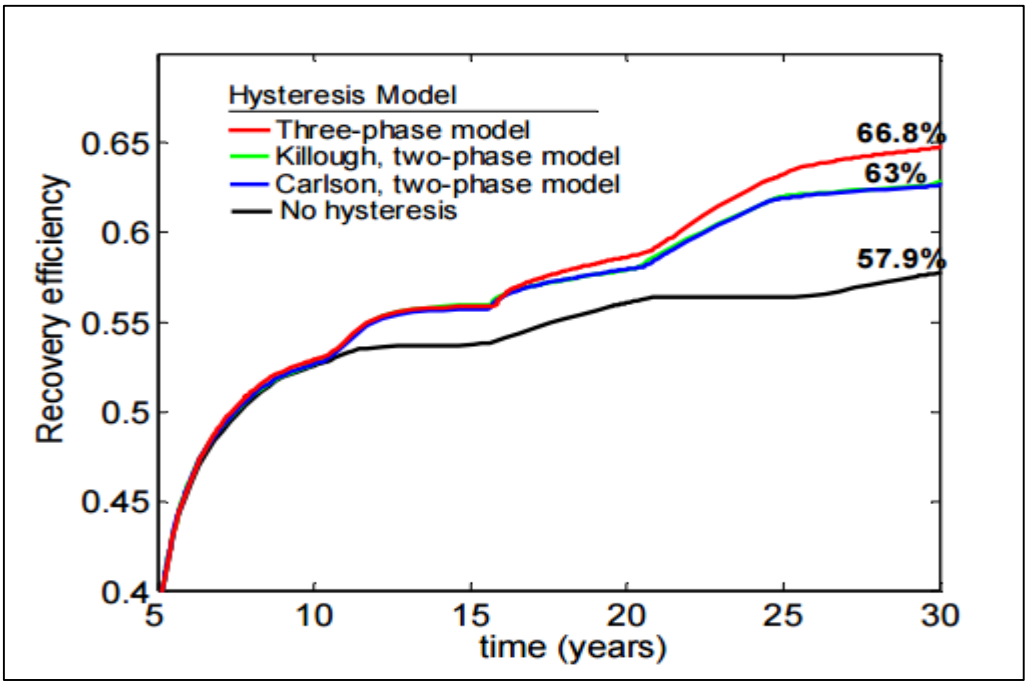

Fig. 2-6 *– Impact of hysteresis model on recovery efficiency (Spiteri & Juanes, 2004).*

2.2 Concepts of WAG

Key aspects of WAG: provide mobility control, improve volumetric sweep efficiency and minimize gravity over-ride effects (Choudhary et al., 2011)

2.2.1 Early History of Wag

Water injection started out in the 1920's. The first systematical approach of waterflooding was first tested in the Bradford field, Pennsylvania (Fettke, 1938). Coincidentally this is also one of the first fields to test out WAG in the mid 1940's, though without crediting the effect to the injected gas. In his investigation of water injection projects, Paul D. Torrey stumbled upon the effect of injecting gas into the reservoir for a period, while otherwise injecting water. The South Penn Oil Company had injected gas in order to have a source of energy surplus they could tap into for a limited time. In retrospect, the effect of the gas injection is quite striking when studying **Fig. 2-7**.

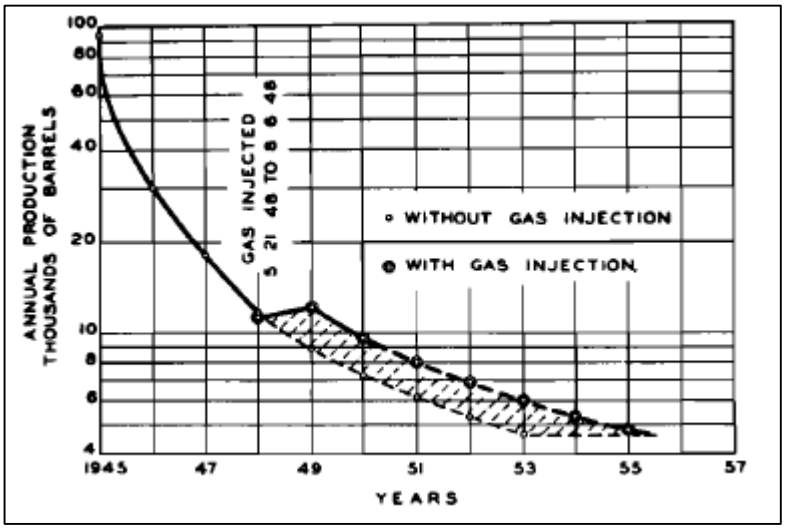

***Fig. 2-7** – Early documentation of production effects due to gas injection following water injection (Torrey, 1951).*

2.2.2 Recovery Mechanisms

2.2.3 Macroscopic Sweep

Macroscopic sweep or volumetric sweep refers to how much of the reservoir volume the displacing fluids manage to cover (Sehbi, Frailey, & Lawal, 2001). Macroscopic sweep is often sub-divided into horizontal sweep and vertical sweep.

For horizontal sweep, the mobility ratio is an important factor. Unfavorable mobility ratio can lead to the displacing fluid fingering the displaced fluid, causing early breakthrough. This is often the case with gas injection due to the low viscosity of gas (Christensen et al., 1998).

Vertical sweep efficiency refers to how much of a vertical cross section is swept by an injected fluid. Due to density differences water will sink as it move towards the producing well. Gas will seek to the top. The vertical sweep efficiency will therefore increase with WAG injection as opposed to only water injection.

In the near well region, three-phase flow will be dominant, see **Fig. 2-8**. The optimal situation during WAG injection is to have the three-phase region extending as far as possible from the injection well bore. The reason for this is that both water and gas relative permeability are reduced in this region, which increases the sweep efficiency.

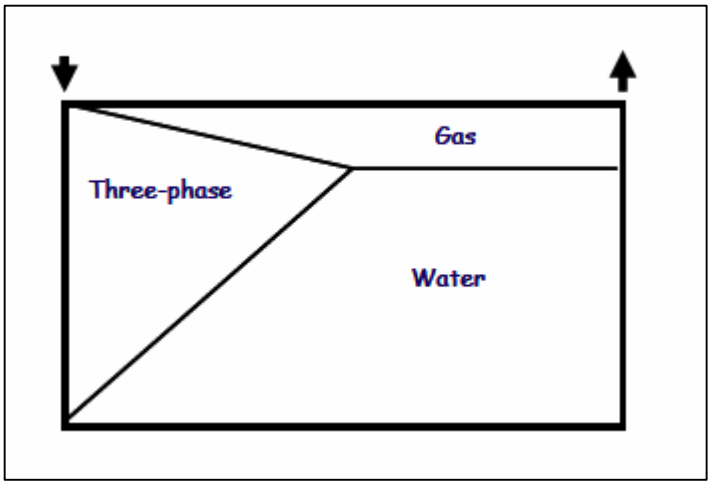

Fig. 2-8 *– Illustration of the different regions during WAG injection (Skauge & Dale, 2007).*

2.2.4 Microscopic Sweep

Microscopic sweep refers to displacement processes on pore scale (Sehbi et al., 2001). Evidence suggests that the introduction of gas in WAG injection relative to only water injection tend to increase the microscopic sweep (Christensen et al., 1998), (Suicmez et al., 2006).

Considering a water-wet system after initial waterflood, the residual oil seek to reside in the largest pores to be furthest away from the rock surface. Injection-gas replaces oil as the most non-wetting, thus pushing oil out from the largest pores. The oil, which probably was poorly connected after the waterflood, is squeezed into smaller pores by the gas. This increases spatial extension of the oil, which makes it possible for oil to increase its connectivity and then be displaced by the second waterflood. This scenario is illustrated in **Fig. 2-9** , which shows pore occupancy plotted in relation to pore size for the saturation path shown in **Fig. 2-10** (Oak, 1990) in (Suicmez et al., 2006).

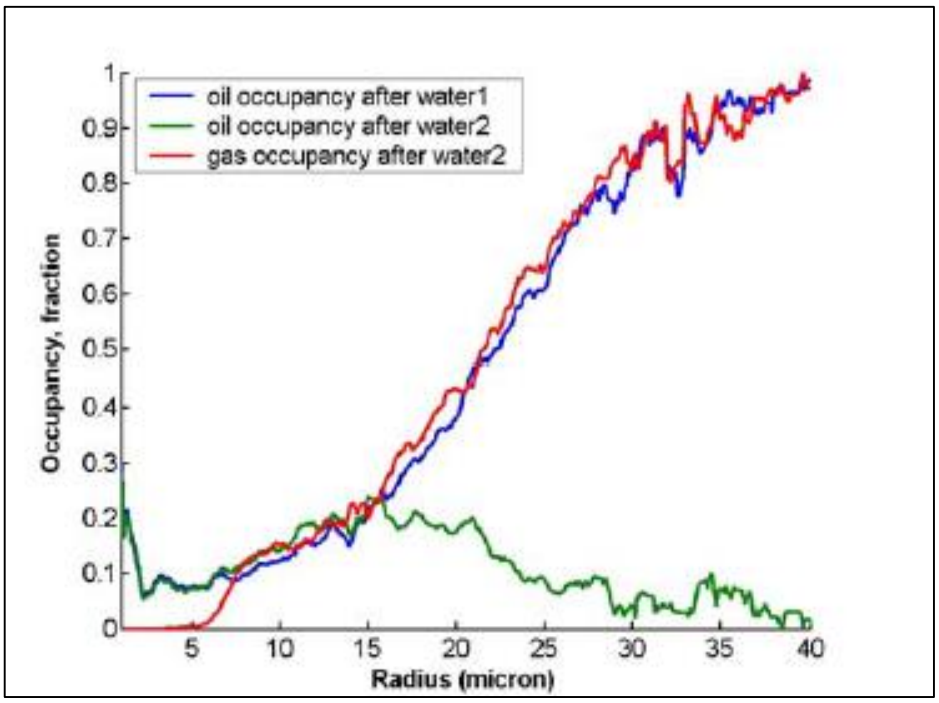

Fig. 2-9 *– Plot showing the microscopic sweep effect of gas . Gas pushes oil out of the larger pores, effectively increasing the oil connectivity due to being pushed into smaller pores. A second waterflood can then displace more of the oil. (Suicmez et al., 2006).*

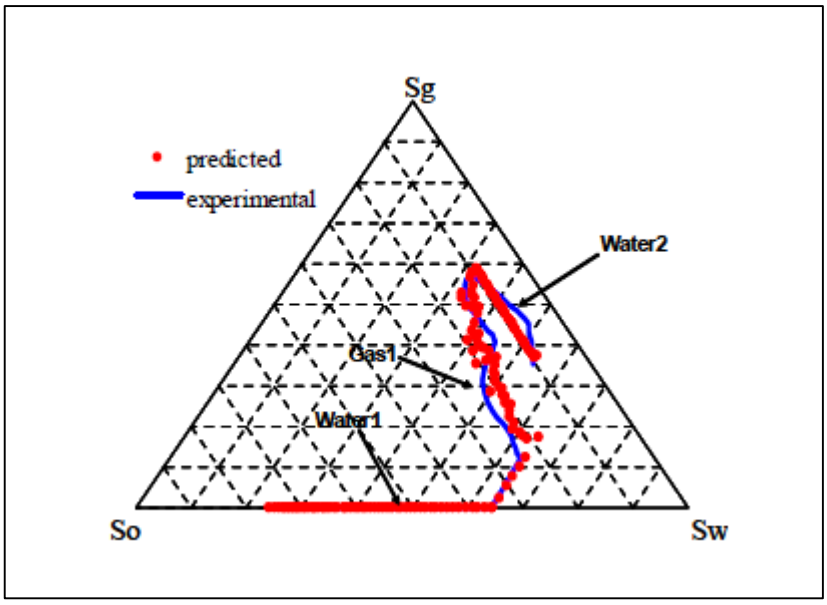

Fig. 2-10 *– Saturation path for water-gas-water injection (Suicmez et al., 2006).*

2.2.5 Compositional Effects of Gas Injection

There are two dominant compositional effects during immiscible WAG injection; **1)** *Swelling*, the process where gas dissolves into oil, and **2)** *Stripping*, the process where components from the oil phase are transferred to the gas phase.

A sensitivity analysis on CO2 injection in the Bakken field reveals that a higher ratio of lighter components in the injection-gas can cause an increase in the ultimate recovery. Injection of pure CO2 results in CO2 dissolving in the oil, while lighter components of the oil are vaporized in order to achieve thermodynamic equilibrium. However, injecting a mix of 50 % CO2, 25 % C1 and 25% C2 (C1 and C2 are lighter than CO2) result in increased stripping of more intermediate components from the oil, as well as the lighter components from the gas are dissolved into the oil. A decrease in density and viscosity of the oil is observed. The reduction of oil viscosity implies an increase in oil mobility, which is beneficial in terms of recovery (Fai-Yengo, Rahnema, & Alfi, 2014)

The study show the importance of injected gas composition and the compositional effects associated with gas injection. Investigation of the severity of the effects is advised with the basis that injected gas should contain a high ratio of the lightest components.

For proper analysis of the stripping effect, compositional simulation is warranted, as black oil simulators are not able to handle this (Petrowiki, 2016).

2.2.6 Gravity Segregation

Due to gravitational forces and density difference, water will eventually sink to lower layers than the one it was injected into. Conversely, gas will only rise to the top. The introduction of injected gas makes it possible to reach oil that is unavailable to water. **Fig. 2-11** illustrate the regions where injection of gas benefits the macroscopic sweep.

Geological heterogeneities could certainly affect the wanted outcome of WAG injection. Low- or non-existing vertical permeability in one or more of the layers could prevent the gas from reaching the top of the formation, thus decreasing the vertical sweep efficiency.

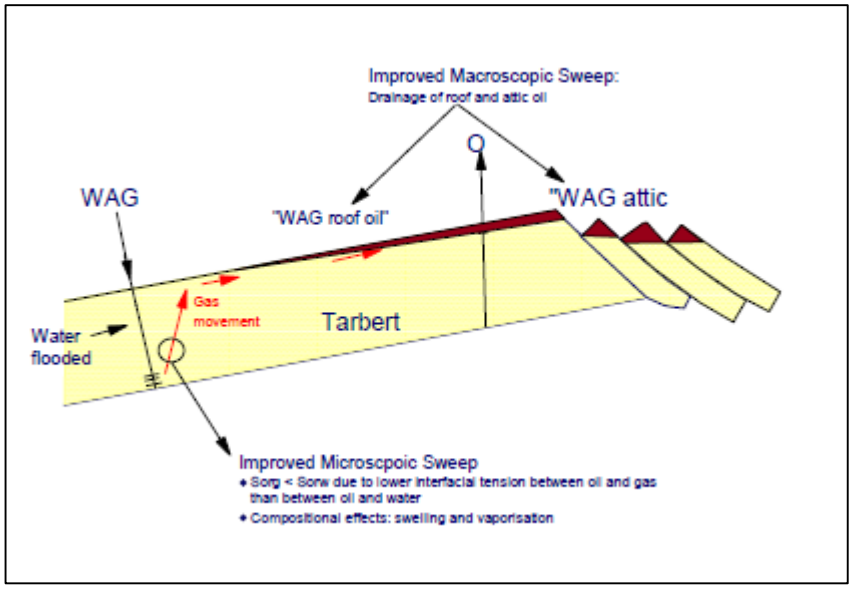

Fig. 2-11 *– Cartoon illustrating the improved recovery due to gas injection in the WAG process (Crogh, Eide, & Morterud, 2002).*

2.2.7 Water Injectivity Limitation

After gas injection, the water saturation near well bore is reduced. This implies reduction in water relative permeability, which then can lead to limited water injectivity (Lien et al., 1998), (Kamath et al., 1998).

2.2.8 Thief Zones

The presence of high permeable layers in the top of the reservoir can reduce the efficiency of the WAG injection. When gas is injected these layers act as thief zones by creating a "highway" for the gas flow. This effect was reported during WAG injection at the Brage field where thin high permeable layers in the Upper Fensfjord formation cause a rapid increase in GOR in the production well (Lien et al., 1998)

3 Simulation Setup

Field scale models are complex and can consist of millions of grid cells. For this reason, a simulation run can take long time to finish. Running compositional three-phase runs increase the complexity and time consumption. A common approach, when one wants to study certain effects without having to wait at length, is to create a simplified model of the region of interest. This chapter provide a short presentation of the simplified model and the field model used in simulations.

3.1 Simplified Model

A simplified model, with two grids, are created to study the effects of WAG within reasonable time. The first grid is a dipping parallelepiped in order to study the effects on roof oil (**Fig. 3-1**). The second is an extension of the first, where a part of the surface has been modified in order to create an area with potential of attic oil (**Fig. 3-2**). A non-permeable zone is modelled in the elevated part of the x- axis, in the middle of the two horizontal producers. This is an attempt to match a similar zone in the field model between A-10 and the other producers shown in **Fig. 3-3**.

The base case for the model is water injection controlled by group voidage from the two injection wells. The base case serves as a reference in order to quantify the incremental recovery of the WAG cases. Model properties and production strategy for the base case can be found in appendix B. The property values are in alignment with those of the field model. STOOIP in the two grids are about a fifth of the field model.

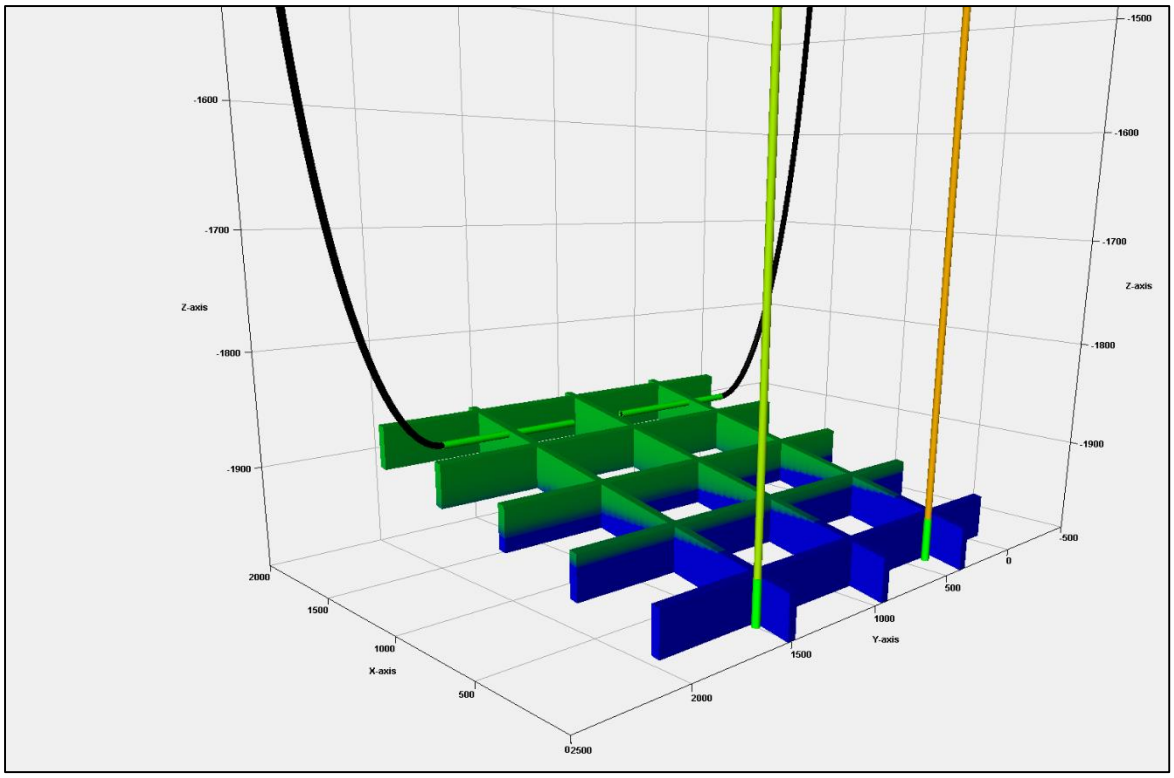

Fig. 3-1 *– Parallelepiped grid. The grid is filtered so the well sections within the reservoir are visible.*

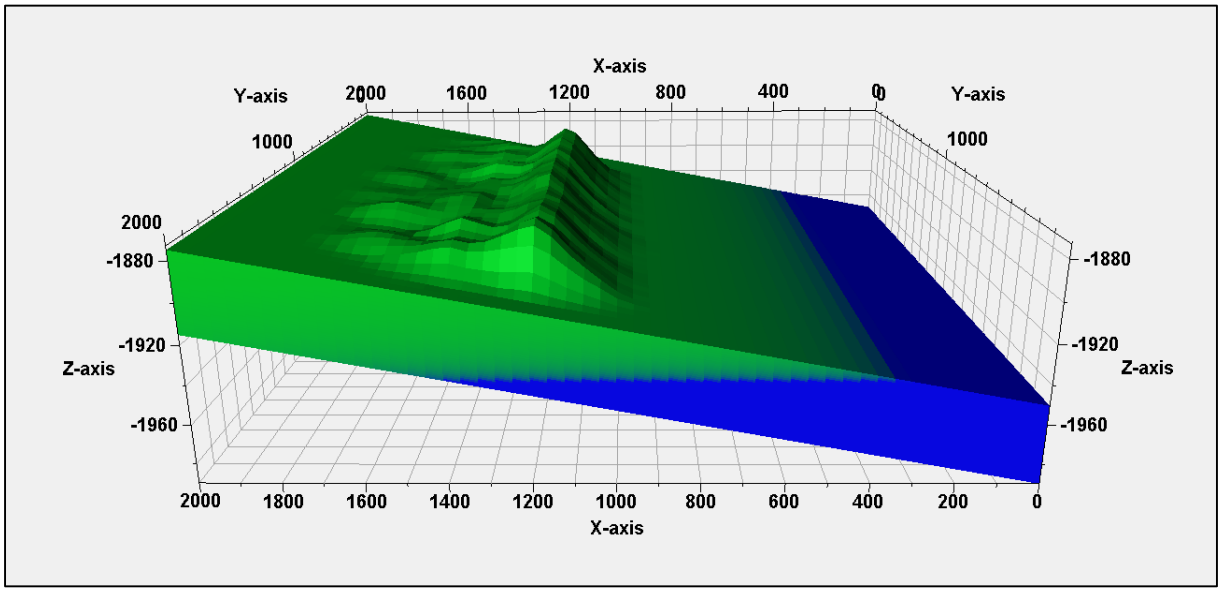

Fig. 3-2 *– Attic grid. The wells are located as shown in* ***Fig. 3-1****.*

3.2 Field Scale Model

A field scale model created for simulation with Eclipse E100, was obtained from the field operator. Modifications were made to the PVT section in order to run the simulation with E300 in compositional mode for the purpose of WAG injection, where proper handling of the compositions is likely to be important. The fluid properties are the same as used in the simplified model and can be found in appendix B.

The model does not include a hysteresis model, as the author did not realize in time that the WAGHYSTR keyword could be used to include hysteresis in the gas phase. The hysteresis effect is shown in the simplified model, which give an indication of the significance of the effect.

Three scenarios were tested:

1) Water injection. This is the default drainage strategy until a study of the EOR potential by WAG injection is completed. WI1 and WI3 opens June 4th 2016 and February 12th 2017 respectively. Other injectors are present, but are not relevant in this paper.
2) WAG injection from WI1 injector with 8 – 4 months WAG cycle, starting with water. WAG injection starts at the same time as start-up of water injection in scenario 1. Gas injection rate is $1 \cdot 10^6$ Sm^3. WAG injection is stopped and water injection is resumed from 01.01.34, to the end of simulation in June 2042, in order to retrieved the injected gas.
3) WAG injection from WI1 and WI3 with 8 – 4 months WAG cycle, starting with water. WAG injection starts at the same time as start-up of water injection in scenario 1. Gas injection rate in each injection well is $1 \cdot 10^6$ Sm^3. The gas injection cycle in the two wells does not coincide. WAG injection is stopped and water injection is resumed from 01.01.34, to the end of simulation in June 2042, in order to retrieve the injected gas. A mistake lead to continuing WAG injection in WI3 to the end of the simulation. This leads to higher volume of gas left in formation.

Fig. 3-3 show the reservoir model with the relevant wells showing. There is a fault located between producer A-06 (red) and A-10 (blue) stretching towards the injection wells less than

half way. This restrict the communication between A-10 and the injectors WI1 and WI2. Gas injection from WI2 would likely follow the same path as gas injected in WI1. This is the reason WI3 is chosen as the next WAG injection well in scenario 3.

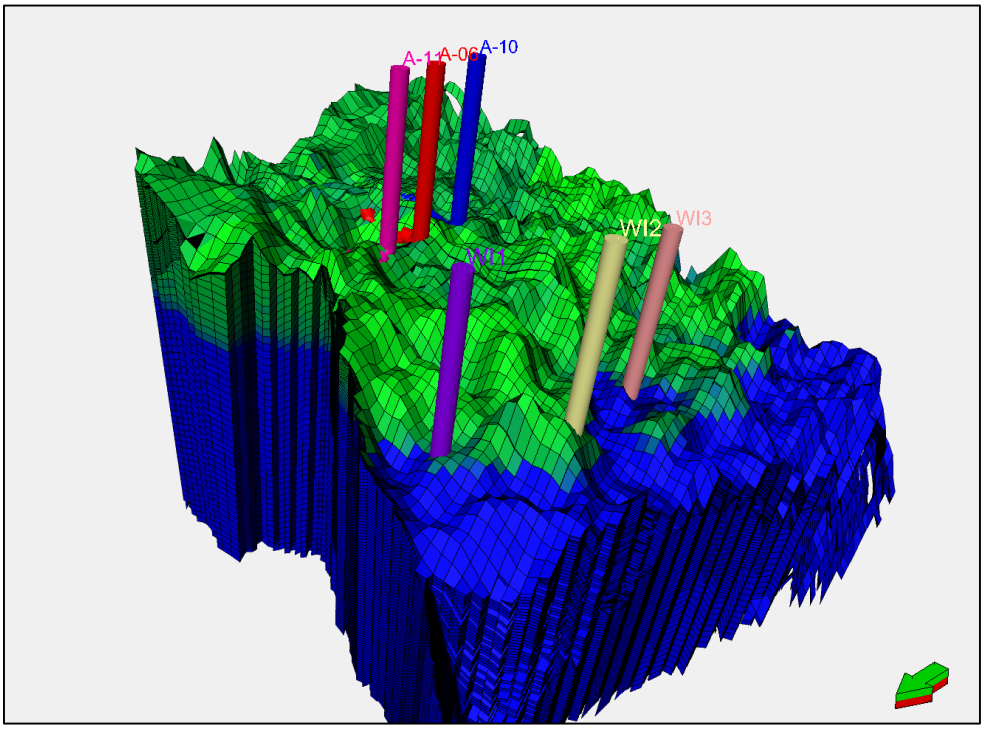

Fig. 3-3 *– Field scale model. The north flank show elevated structures that gives rise to WAG potential.*

4 Results

4.1 Simplified Model Results

Sections 4.1.1 – 4.1.3 are based on the box model, while sections 4.1.4 - 4.1.6 are based on the attic model.

4.1.1 Cycle Length Sensitivity

The length of water and gas cycles is a parameter that is of interest during a WAG injection process. To see how different cycle lengths affect the production and GOR four cases was tested. In **Fig. 4-1** it can be observed that while cumulative production show only a slight increase when for longer gas cycles, the GOR is much higher. This indicates that it longer gas cycles cause more problems that the potential benefit of increased recovery.

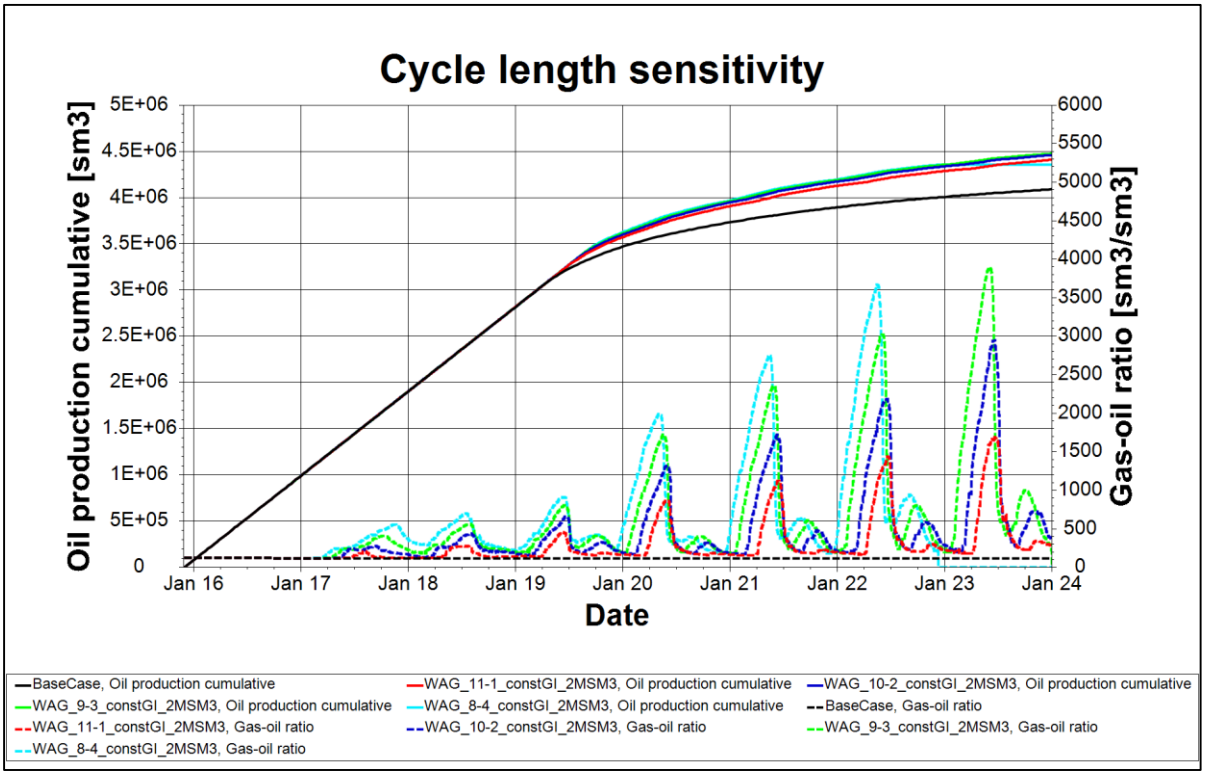

Fig. 4-1 *– Cumulative oil production and gas-oil ratio for different cycle lengths ; 11 months water and 1 month gas (red), 10-2 (blue), 9-3 (green) and 8-4 (light blue). This is for production well OP1. Note that for the 8-4 simulation the well shuts-in early.*

4.1.2 Gas Injection Rate Sensitivity

Higher initial gas injection rate increase the extension of the three-phase zone. As the three-phase zone leads to lower final oil saturation, increase in oil recovery is expected. **Fig. 4-2** show cumulative oil production and GOR for three different gas injection rates. It is evident that the GOR is affected much more than the incremental oil recovery. A doubling of the injection rate leads to approximately a doubling of the GOR, while it only leads to a slight increase in the incremental oil recovery.

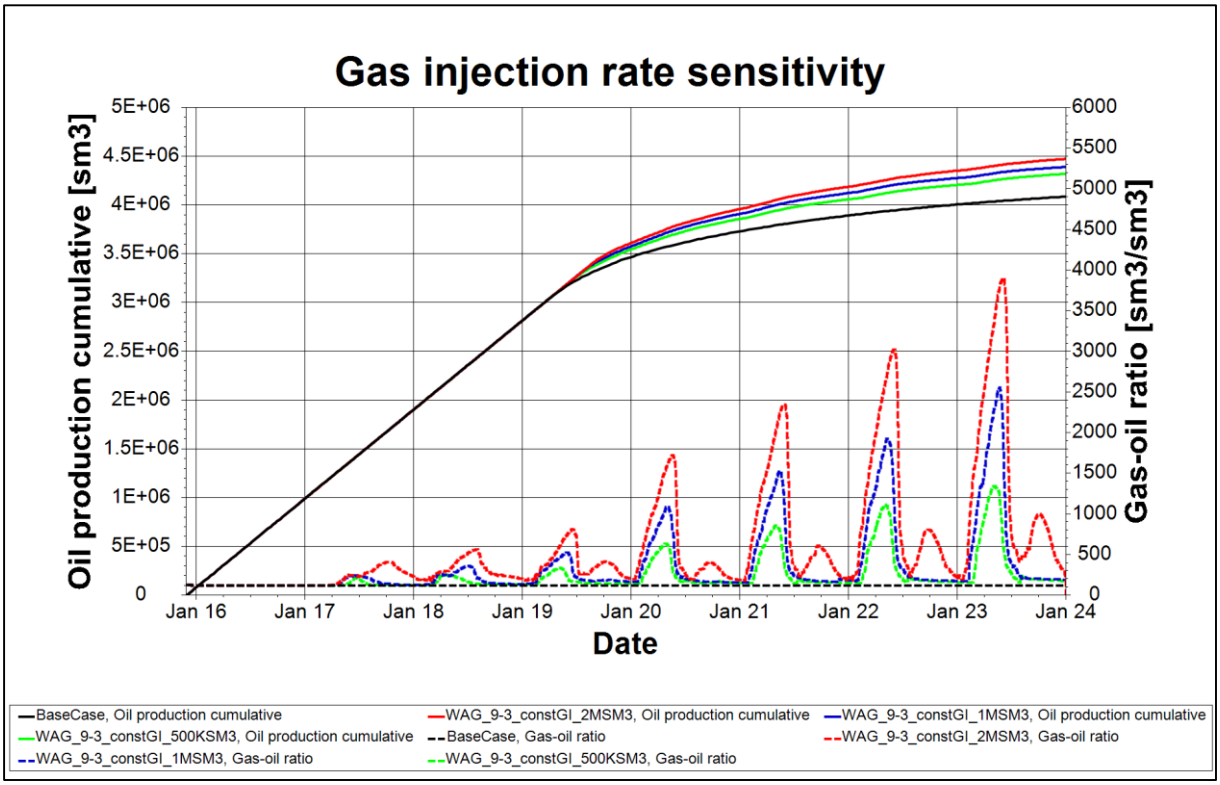

Fig. 4-2 *– Cumulative oil production and gas-oil ratio for base case and WAG injection with constant gas injection rate of; 2 · 10^6 Sm^3/day (red), 1 · 10^6 Sm^3/day (blue), 0.5 · 10^6 Sm^3/day (green) throughout the simulation runs.*

4.1.3 Gas Injection Restricted Based on Production Oil Rate

Constant gas injection rate throughout the entire life of the field leads to increasingly high gas-oil ratio, up to extreme values. High GOR is concerning cause it could limit the oil

production if gas-processing capacity on the production platform is limited. From the constant gas injection simulation runs it can be observed that GOR changes the rate of increase at the end of the production plateau. In order to maintain a more stable GOR a gas reduction strategy is tested. The strategy simply calls for a reduction in the gas-injection rate proportionally to the decrease in oil production rate. By using the ACTIONX keyword in eclipse it was specified that when production oil rate went below plateau production rate at 5000 Sm^3 gas injection rate was set to a factor of 0.9 of initial. Then for every 500 Sm^3 decrease in oil production rate, the reduction factor was decrease with 0.1.

Fig. 4-4 compares the constant gas injection case to the strategy outlined above. Gas injection rate can be seen in **Fig. 4-3**.The reduction strategy leads to a more balanced GOR after plateau, while the ultimate cumulative oil production is only slightly reduced.

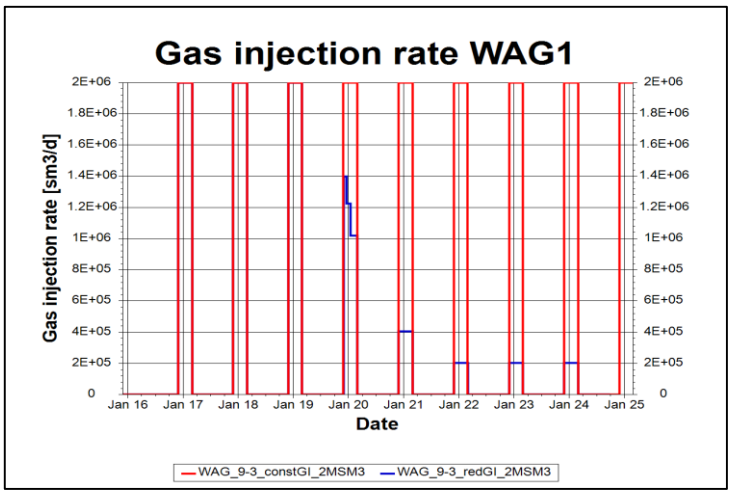

Fig. 4-3 *– Gas-oil ratio for constant and restricted gas injection cases.*

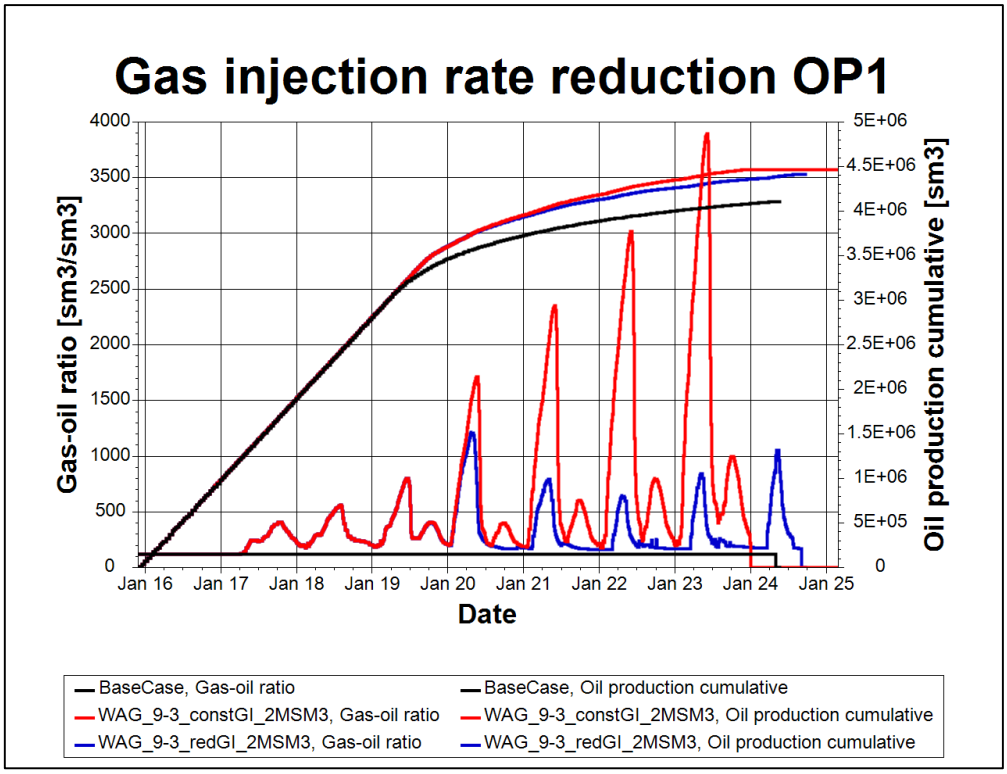

Fig. 4-4 *– Result of reducing the gas injection proportional to the decline in oil production rate.*

4.1.4 Effect of Gas Trapping Model in Simulation

Gas trapping greatly affects the oil recovery as can be seen in **Fig. 2-4**. By using the WAGHYSTR keyword in eclipse, hysteresis for the gas phase can be included in the simulation, even without the imbibition curve. While eclipse expects an imbibition curve when hysteresis option is activated in SATOPTS, the WAGHYSTR keyword calculates the imbibition curves from the drainage curve. Thus, inserting a copy of the saturation function used in SATNUM into IMBNUM as a placeholder, Eclipse is satisfied and gas trapping can be simulated without the additional IMBNUM input.

Table 1 show incremental recovery in cases with and without gas trapping hysteresis for 8-4 cycle with gas injection rate of $2 \cdot 10^6$ Sm^3/day. When hysteresis is accounted for, this causes higher increase in incremental oil recovery. It also leaves more gas in the reservoir, which is important to account for when we think about the overall energy extraction. Energy from gas can be converted into oil equivalents. 1000 sm3 gas equal 1 SM3 oil equivalent in energy terms. Looking at the incremental increase in oil equivalents we get a picture of how much

additional energy is recovered due to the WAG injection. The incremental increase in oil equivalents for the hysteresis case is about a half of the incremental oil increase and about 2/3 of the oil increase in the non-hysteresis case.

Plots showing cumulative oil production, oil production rate and GOR can be found in **Fig. A-14** through **Fig. A- 16** in appendix.

Table 1 *– Incremental recovery for cases with and without the hysteresis option.*

Scenario	Recovery factor	Increase oil [%]	Increase in oil equivalents [%]	Gas left in reservoir [10^6 Sm^3]
Base case	0.620			
NOHYST	0.680	9,65	7,54	96,0
HYST	0.697	12,43	6,21	282,5

4.1.4.1 Gas Saturation and Relative Permeability

During WAG injection, gas is trapped in the larger pores after the second water cycle. This effect is not accounted for when hysteresis option is not selected and this leads to large fluctuations of the gas saturation as can be seen in **Fig. 4-5**. When gas-trapping hysteresis is included, the trapped gas maintains the overall gas saturation at a high level, while it fluctuates above the trapped gas saturation when additional gas is injected.

"Trapped" gas saturation, implies that this saturation is not mobile. This affects the gas relative permeability as can be seen in **Fig. 4-6**.

The gas saturation and relative permeability profiles are from grid block (15, 12, 4). This grid block is located in the three-phase zone. The location of the grid block, as well as similar profiles for oil and water and illustrative cross-sections can be found in the appendix, **Fig. A-1** to **Fig. A- 11**.

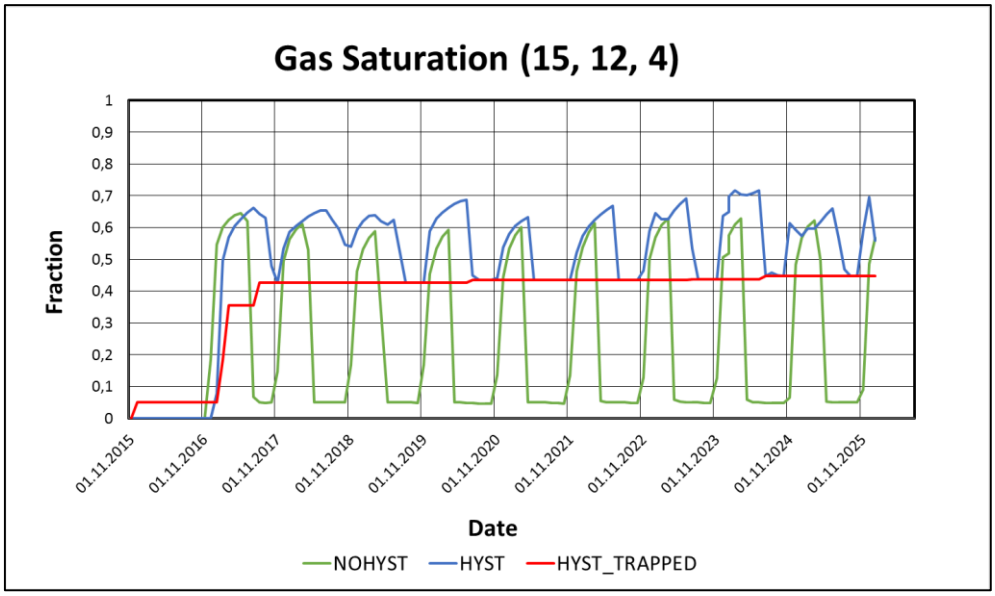

Fig. 4-5 *– Gas saturation in grid block (15, 12, 4) for cases with and without gas-phase hysteresis.*

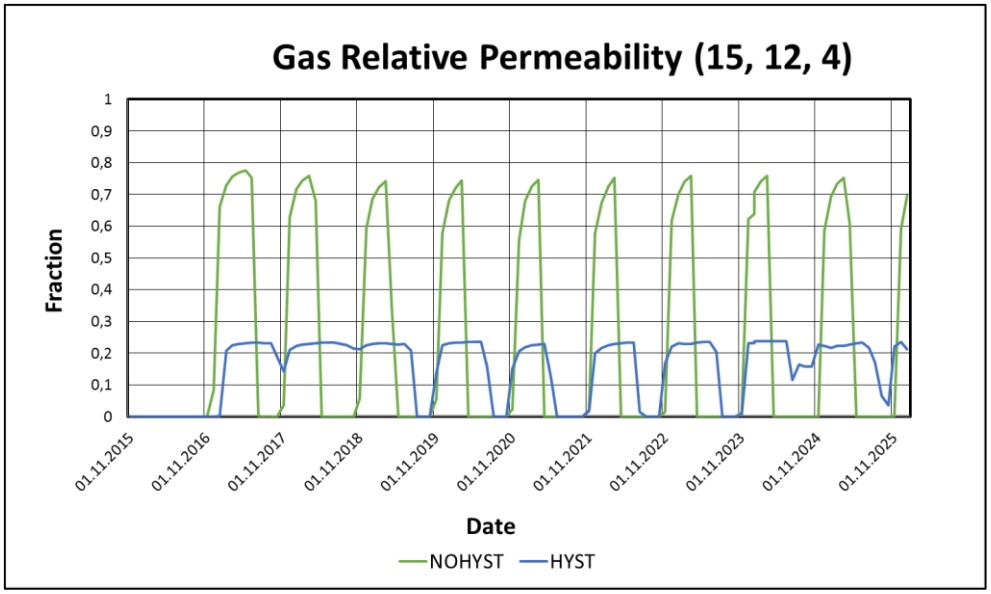

Fig. 4-6 *– Gas relative permeability in grid block (15, 12, 4) for cases with and without gas-phase hysteresis.*

4.1.4.2 Water Injectivity Limitation

Decreased water relative permeability in the three-phase zone (**Fig. A- 9**) might decrease the injectivy of water. Water injection is supposed to make sure that injected reservoir volume rate equals produced reservoir volume rate (voidage) in order to maintain approximately constant pressure. By comparing injected and produced reservoir volume rate, it can be observed that when production suddenly increases due to the water breakthrough, the injection of water does not manage to follow the rate increase, **Fig. 4-7**.

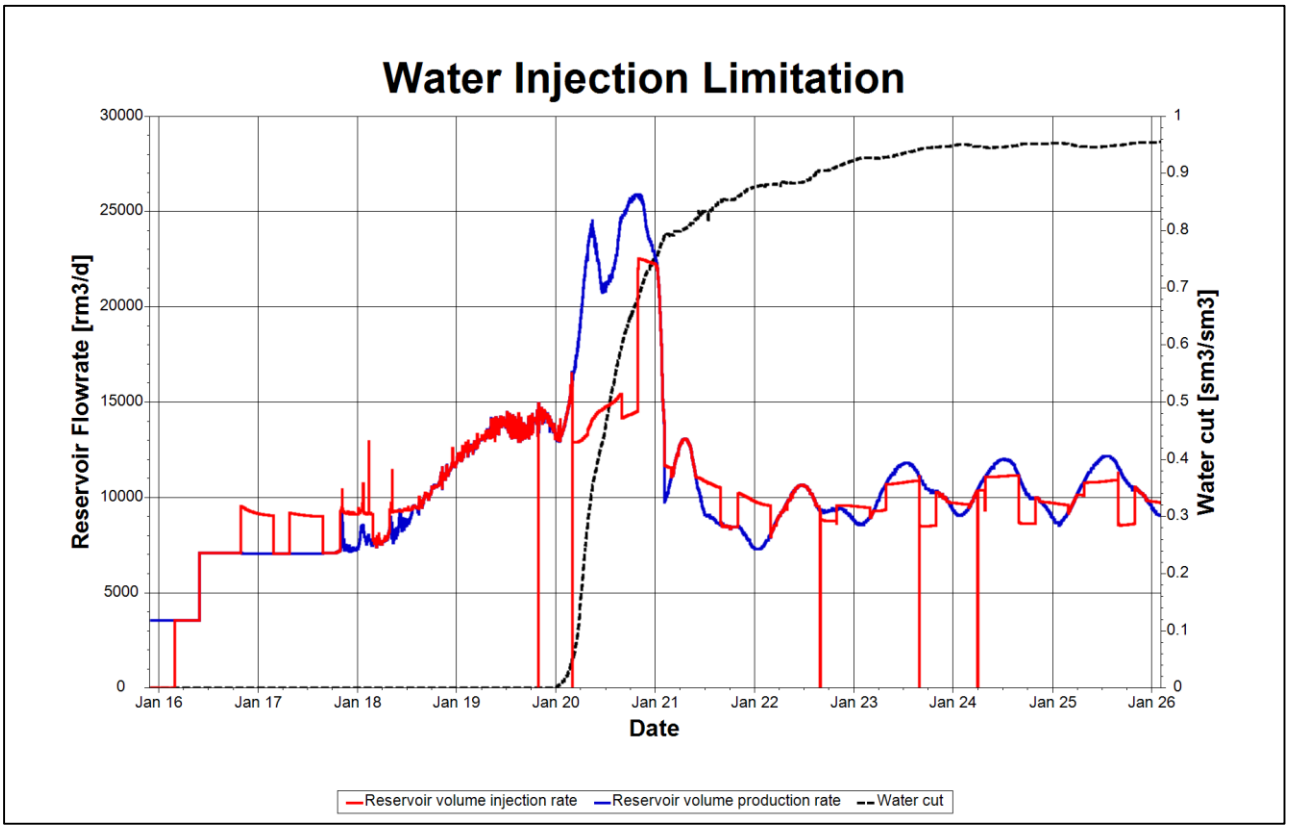

***Fig. 4-7** – Field production (blue) and injection (red) reservoir volume rate for case with gas-phase hysteresis.*

4.1.5 High Permeable Top Layer

The presence of high permeable layers in the top of the reservoir in the region between a WAG injection well and its corresponding producer(s) might be detrimental to the WAG injection process. The grid was modified such that the horizontal permeability of the top layer was increased by a factor of 10. Gas trapping is included. **Fig. 4-8** show trapped gas saturation approximately three years after first gas cycle. The three-phase zone and the gas accumulation in the superstructure is significantly reduced in the presence of a high permeability top layer at this time. **Fig. 4-9** show tertiary saturation. Observe that the water, as well as the gas, prefers the top layer, thus decreasing the sweep efficiency in the lower parts of the reservoir.

In **Fig. 4-10** through **Fig. 4-12** it can be observed that the oil production starts declining at the same time as the base case, but it maintain a higher production towards the end of the simulation. The GOR starts out higher for the high perm case, but does not increase at the same rate as the homogenous case. It does however increase more suddenly than for the homogenous case. As the simulation is not completed, it is too soon conclude about ultimate recovery.

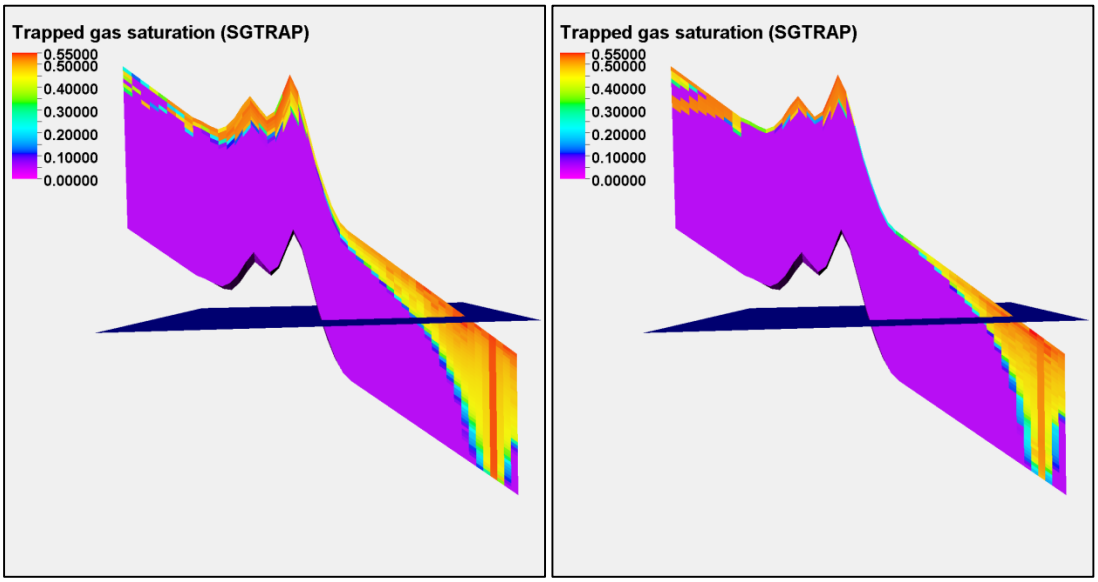

Fig. 4-8 *– Trapped gas saturation. Lands trapping coefficient, C = 0.7. Homogenous reservoir to the left and high permeable top layer to the right. The horizontal plane show the water-oil contact. Date: 28.12.19*

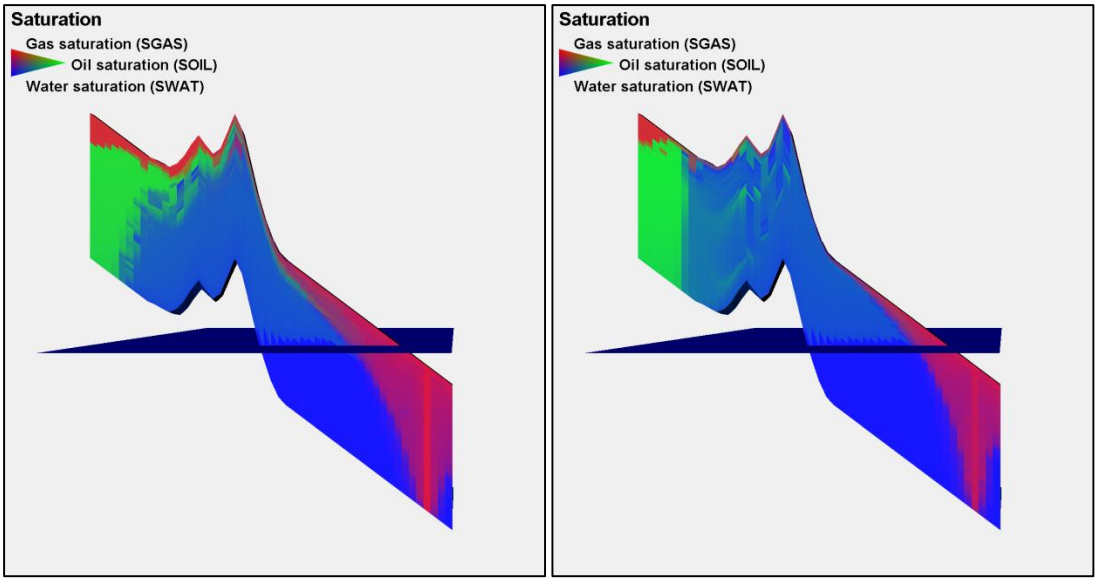

Fig. 4-9 *– Water, oil and gas saturation. Homogenous reservoir to the left and high permeable top layer to the right. Date: 28.12.19*

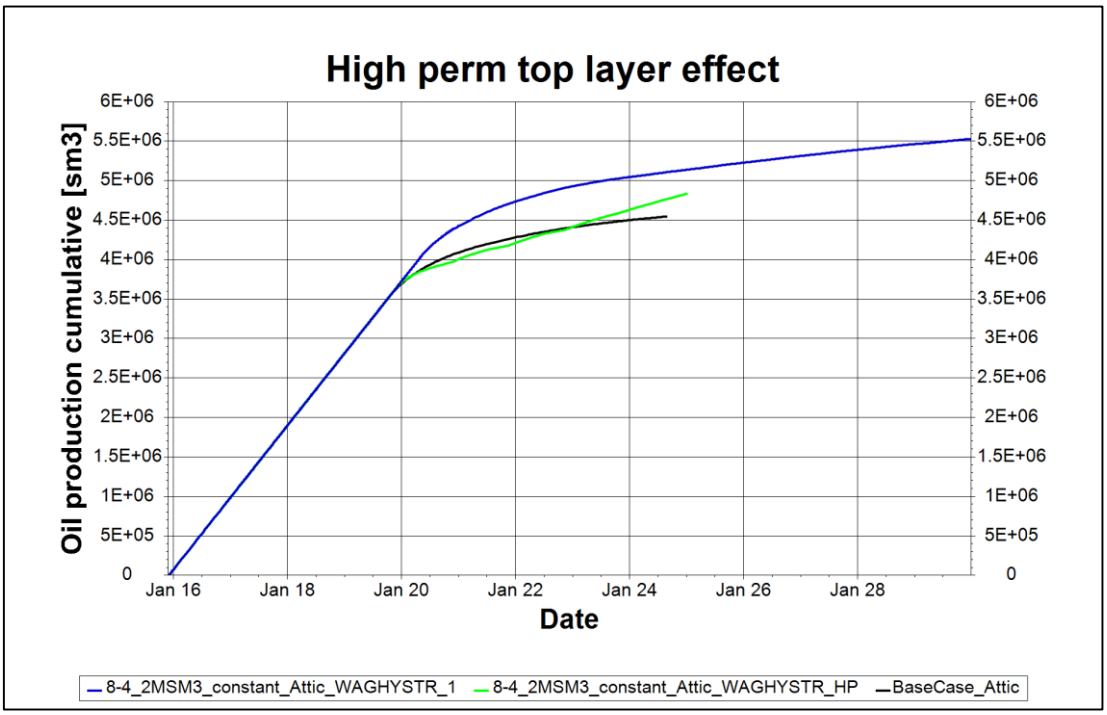

Fig. 4-10 *– Cumulative oil production for homogenous (blue) and high permeability top layer (green) model. The high perm case starts declining at the same time as water injection, but maintain a higher production rate towards the end. Note that the simulation for the high perm case is not completed.*

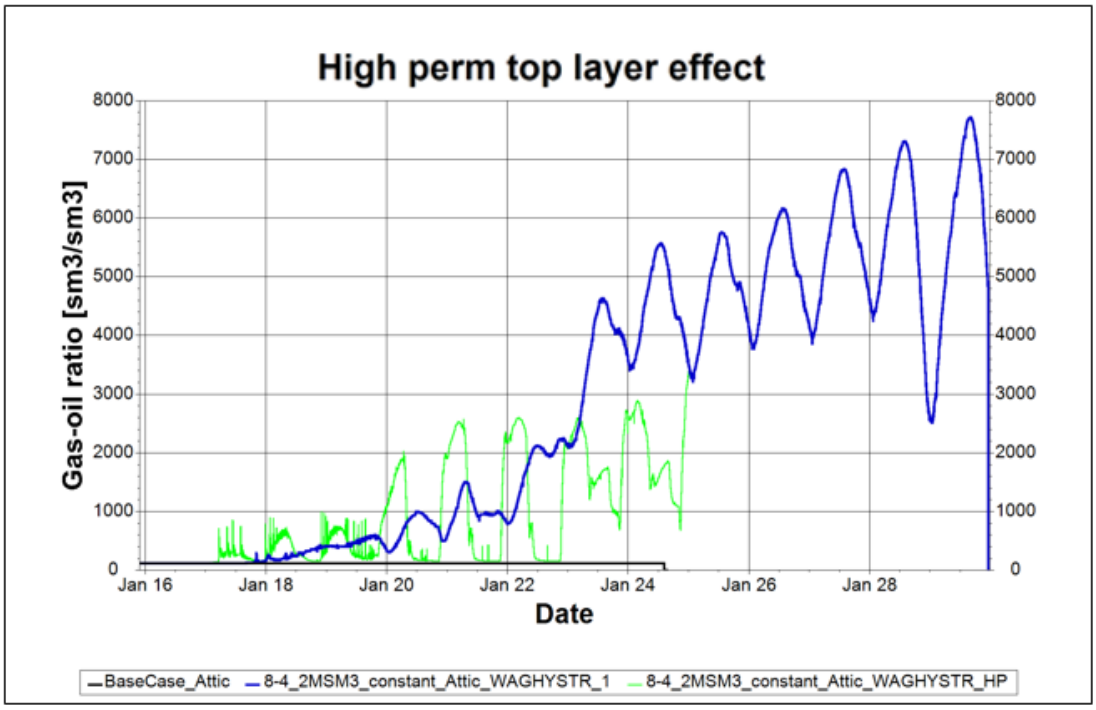

Fig. 4-11 *– GOR for homogenous (blue) and high permeability top layer (green) model.*

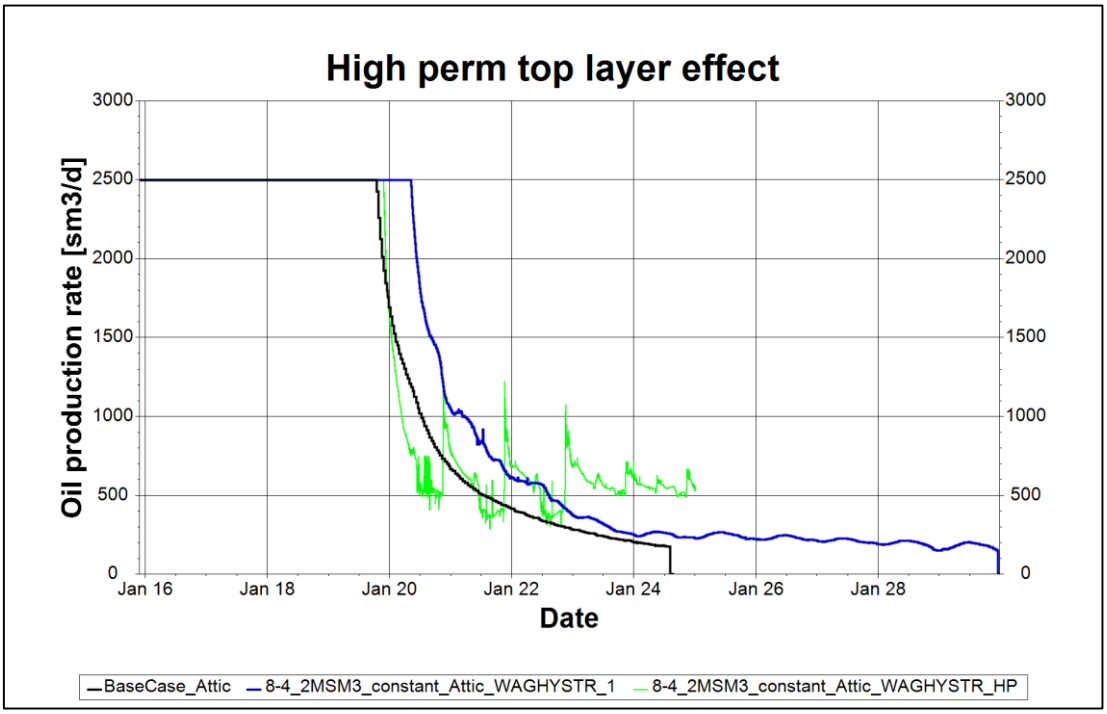

Fig. 4-12 *– Oil production rate for homogenous (blue) and high permeability top layer (green) model.*

4.1.6 Compositional Effects

As the oil is exposed to the injection-gas, interchanging of components start to occur. This affects the density and viscosity of the oil. Density and viscosity in the vicinity of the three-phase zone plotted versus time can be seen in **Fig. 4-13** and **Fig. 4-14**. The decrease in density indicate that the oil phase has either received lighter components from the gas, been stripped from intermediate components, or most probably, both. The decrease in viscosity causes an increase in the mobility of the gas. In **Fig. 4-14** gas saturation for the grid blocks, where gas is actually present, is included. This shows that the compositional effects also affect grid blocks that are located some distance away from the three-phase zone.

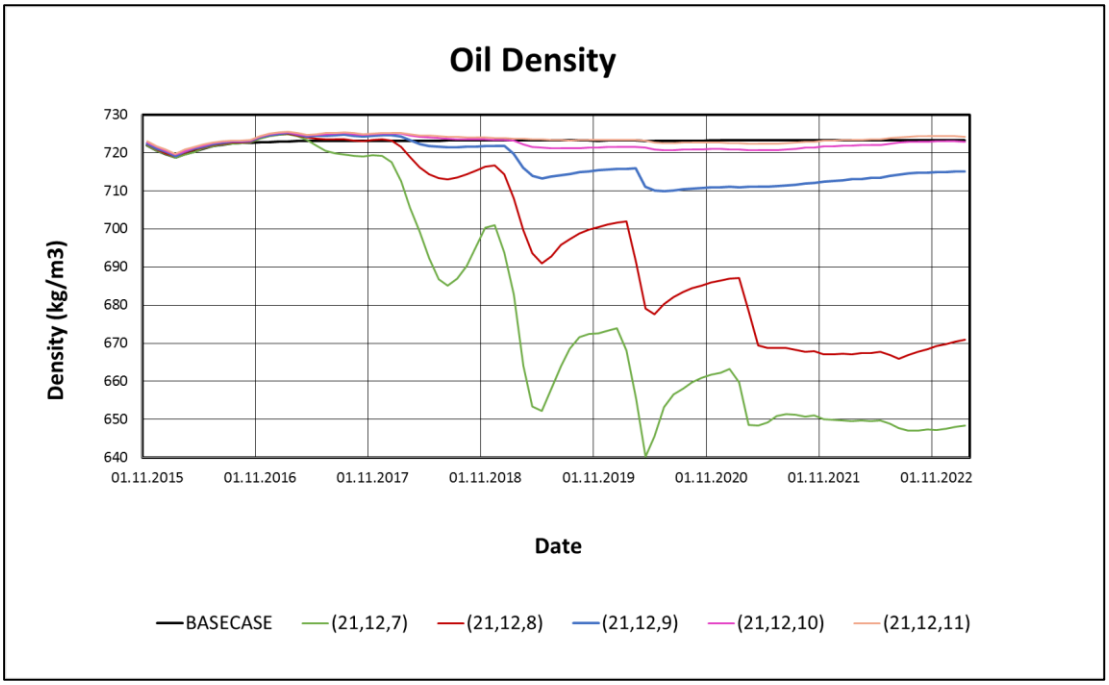

Fig. 4-13 *– Oil density for different grid blocks in the boundary of the three-phase region. Indicates stripping/swelling effects.*

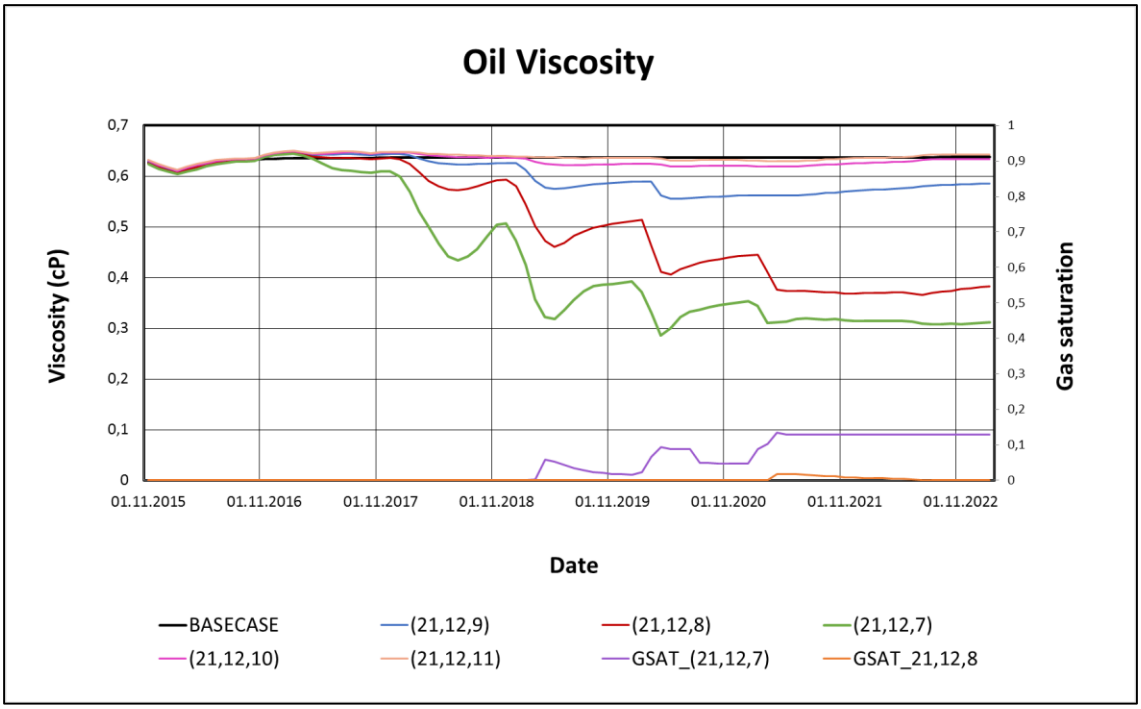

Fig. 4-14 *– Oil viscosity for same grid blocks as in* ***Fig. 4-13****. Gas saturations for the grid blocks that are in the three-phase zone is included.*

4.2 Field Scale Results

4.2.1 Gas Migration 3D

Fig. 4-15 show tertiary saturation 10 years after field start-up. The main objective with this figure is to show the pathway of the injected gas. Gas moves along the most elevated areas in the reservoir due to gravitational forces that pushes it upwards. Between WI1 and A-11 the gas follows the boundary of the reservoir.

The gas injection from injector WI3 establish a preferred path to A-10. There is increased potential if the gas had also established contact with the OP9B producer. In this simulation, OPB9 starts production only half a month before the first gas cycle from WI3. This may have be one reason for the lack of contact. One can also consider increasing the gas injection rate in hope that a connection could be established. It might also be that the permeability between WI3 and A-10 is higher.

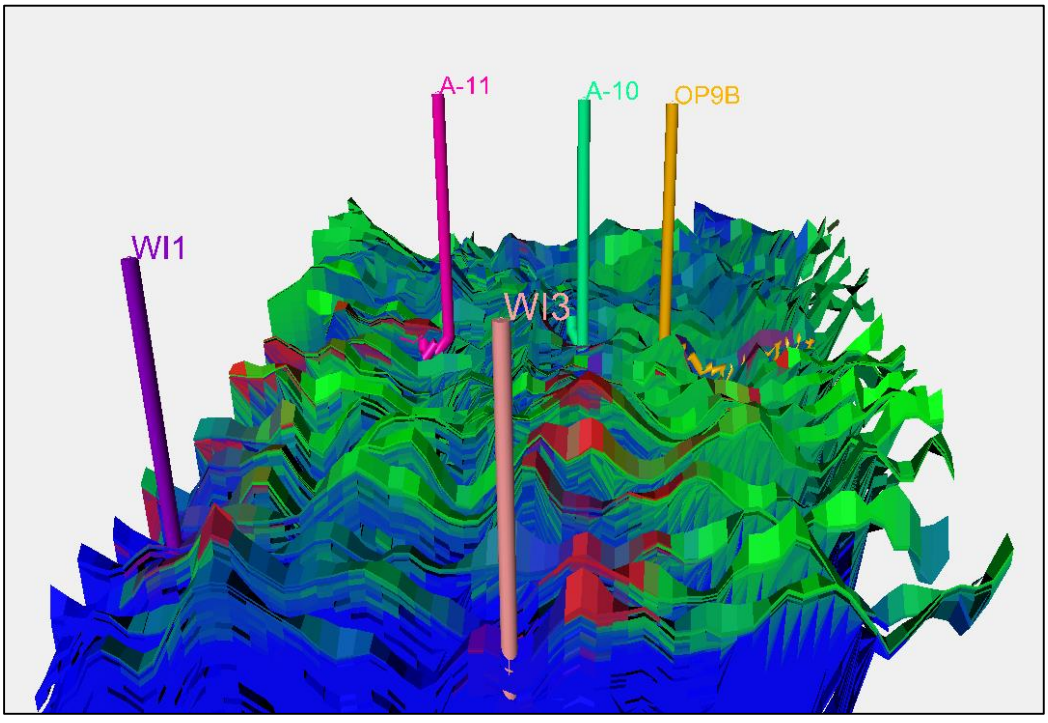

Fig. 4-15 – *Tertiary saturation of the reservoir 10 years after of start-up.*

4.2.2 2D View of Gas Migration from Injector WI1 to Producer A-11

Fig. 4-16 illustrate the gas migration form WI1 to A-11. A cross section was created in order to be able to show the vertical sweep of the WAG injection. The path of the cross section was chosen in order to shed light on the elevated structures that can be seen in ***Fig. 4-15***.

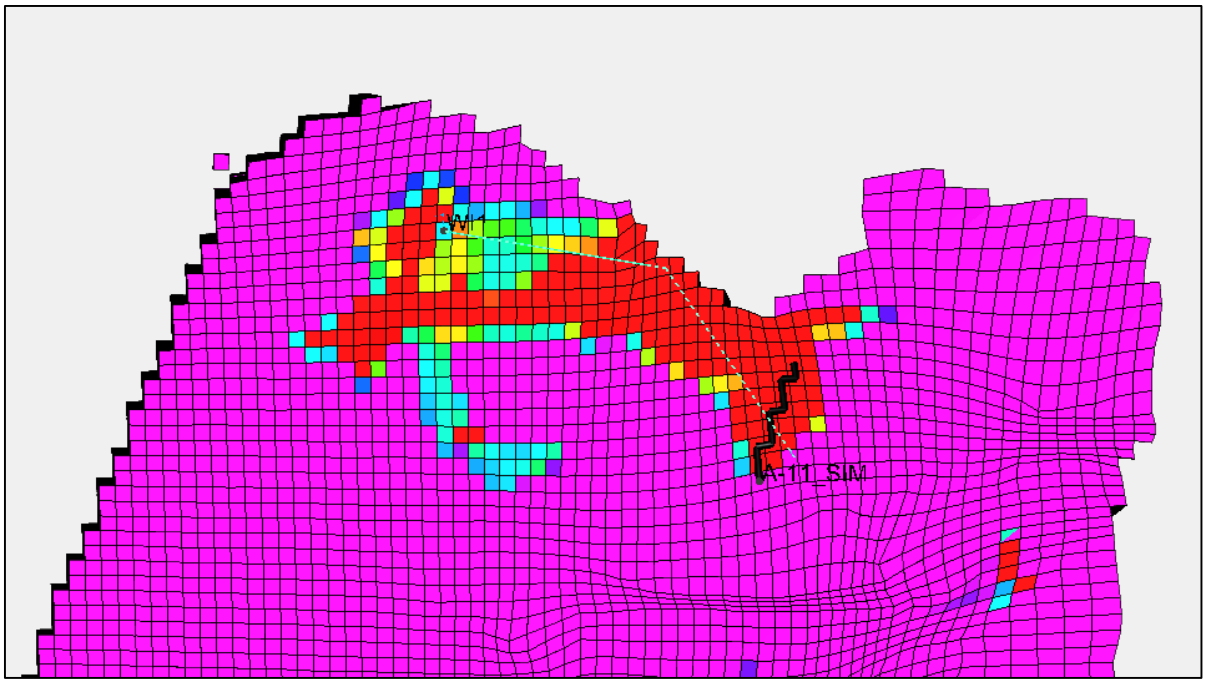

Fig. 4-16 *– 2D view of region between injector WI1 and producer A-11. This illustrates the direction of the gas migration. The line in the figure is used to create the cross sections in the following figures.*

4.2.3 Gas Saturation

Fig. 4-17 and **Fig. 4-18** show gas saturation for different scales. **Fig. 4-17** show gas saturation with a low interval scale. The focus is to show all areas that are affected by the gas. Investigation of the figure reveals that gas follows the path of a fault in the reservoir. This restricts the horizontal evolution of the three-phase saturation region. **Fig. 4-18** show the accumulation of gas in the top part of the reservoir. High gas saturations imply great sweep efficiency of the gas.

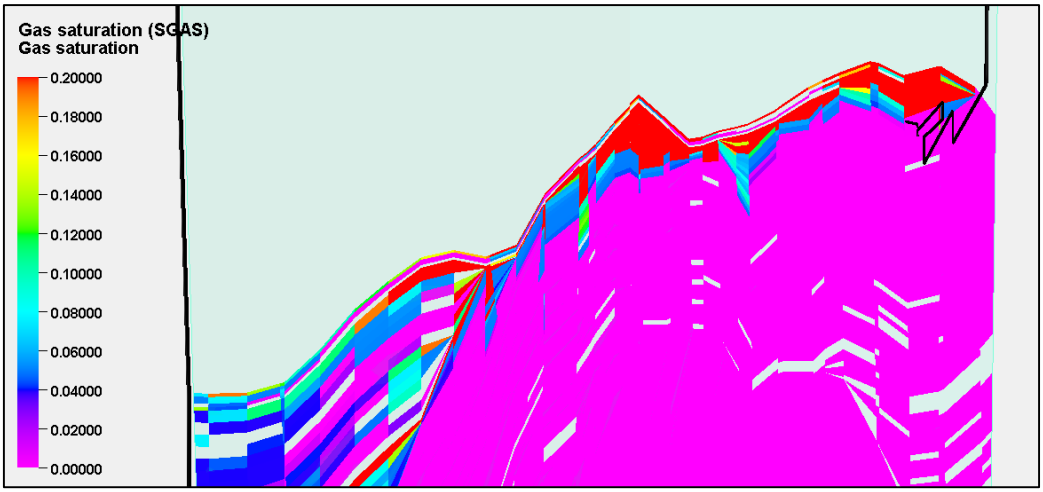

Fig. 4-17 *– Gas saturation at the end of WAG injection with low interval scale. Date: 01.01.34*

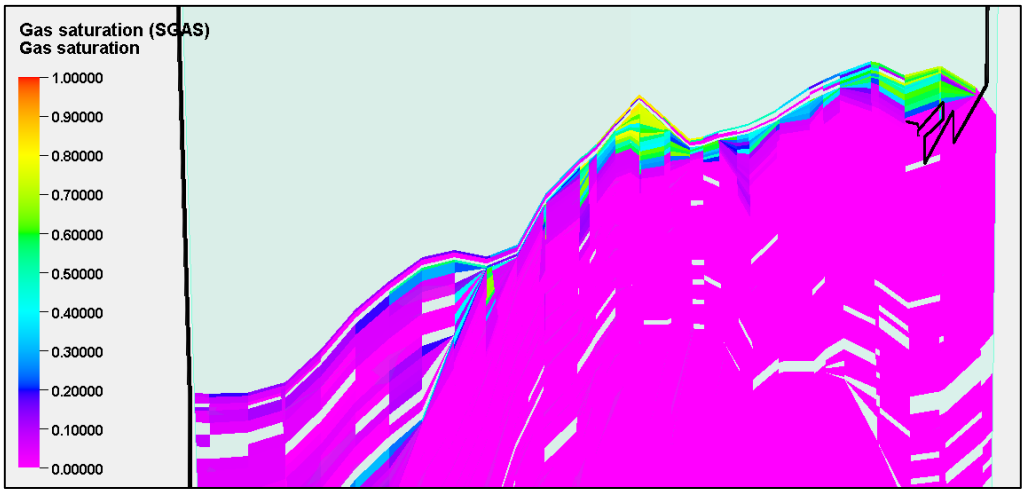

Fig. 4-18 *– Gas saturation at the end of WAG injection with full range scale. Date 01.01.34*

4.2.4 Decrease in Oil Saturation

Comparing the sweep efficiency of water injection to WAG injection is done by investigating the decrease in oil saturation. **Fig. 4-19** and **Fig. 4-20** show the difference in oil saturation, from start to end of WAG injection, for the cross section shown in **Fig. 4-16**. It is evident that the WAG injection increases the vertical sweep due to the gas injection, which effectively sweeps the top of the reservoir. In addition, increased recovery can be seen near the injector.

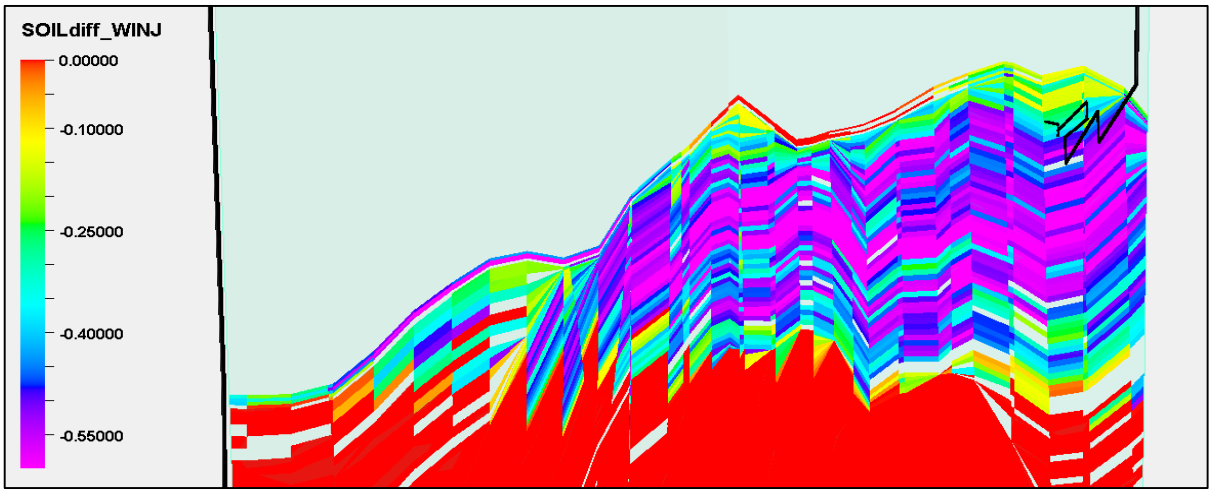

Fig. 4-19 *– Difference in oil saturation from initial conditions to 01.01.2034 for scenario 1 (water injection). Note the negative scale. Observe that the waters ability to sweep the top part of the reservoir is rather poor.*

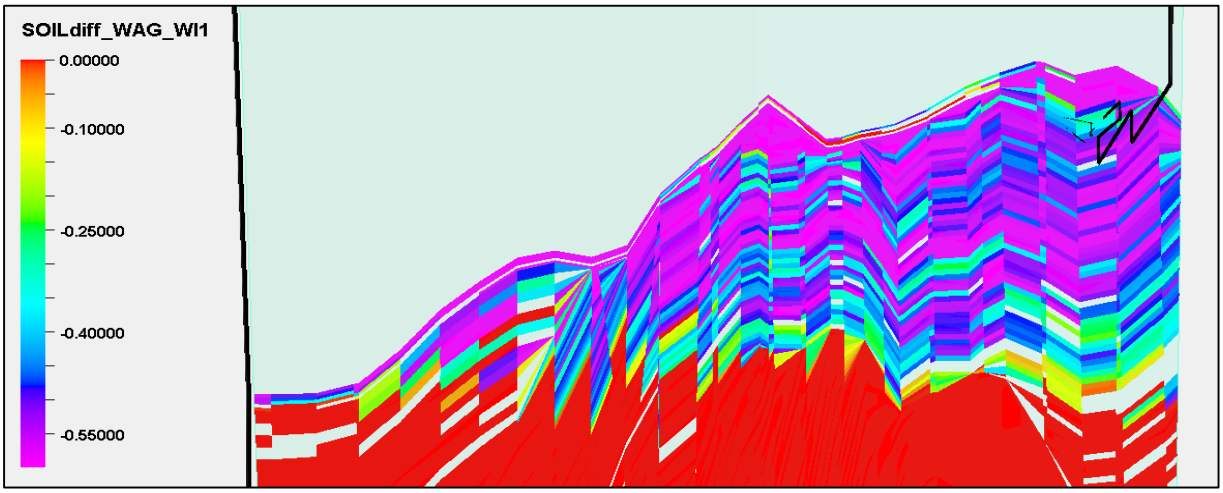

Fig. 4-20 *– Difference in oil saturation from initial conditions to 01.01.2034 for scenario 2. Note the negative scale. Higher decrease in oil saturation at the top of the reservoir illustrate how gas effectively increase the total volumetric sweep. The combination of gas and water also increase the sweep near the injection well bore.*

4.2.5 Summary Results

This section provides summary results of the three scenarios that has been tested in the field scale model.

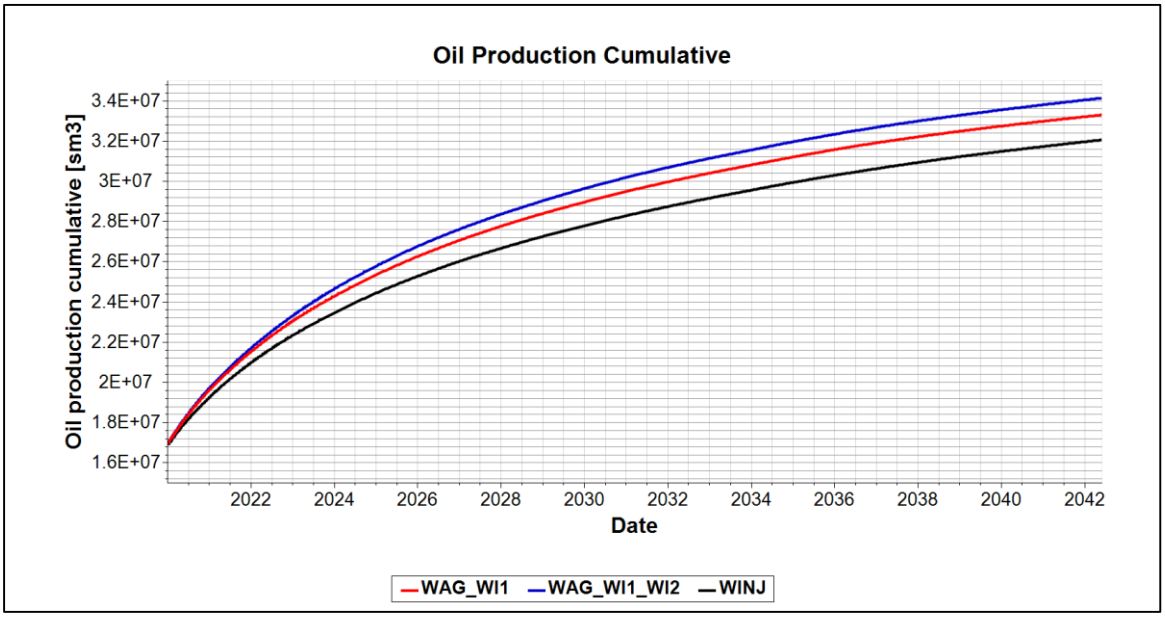

Fig. 4-21 *– Cumulative oil production for field*

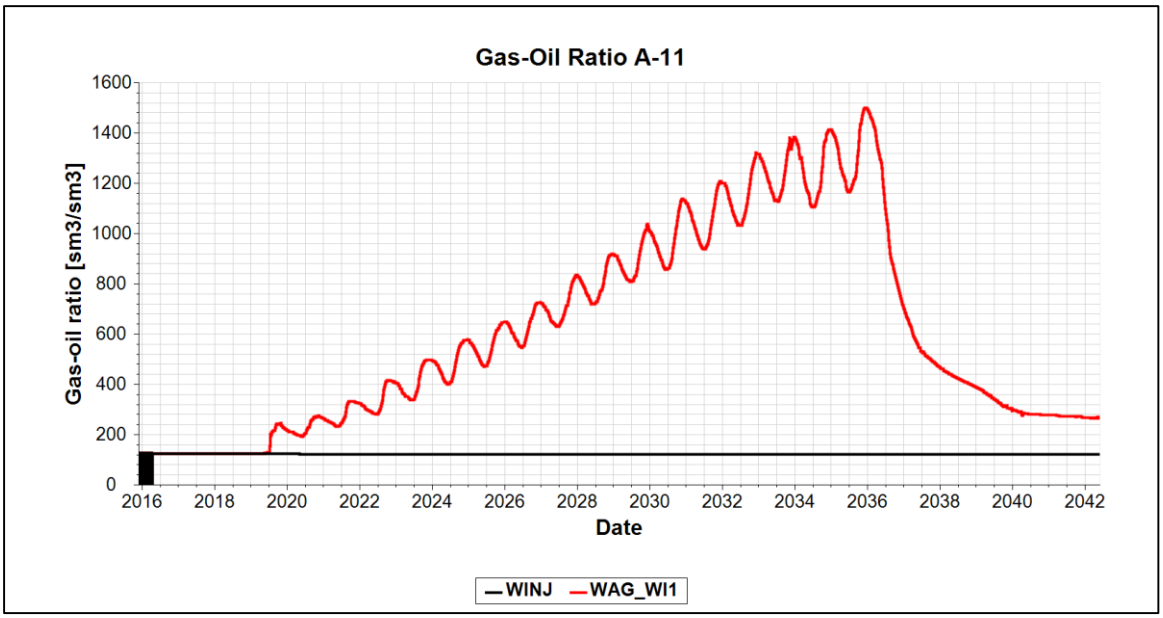

Fig. 4-22 *– Gas-oil ratio for wells A-11.*

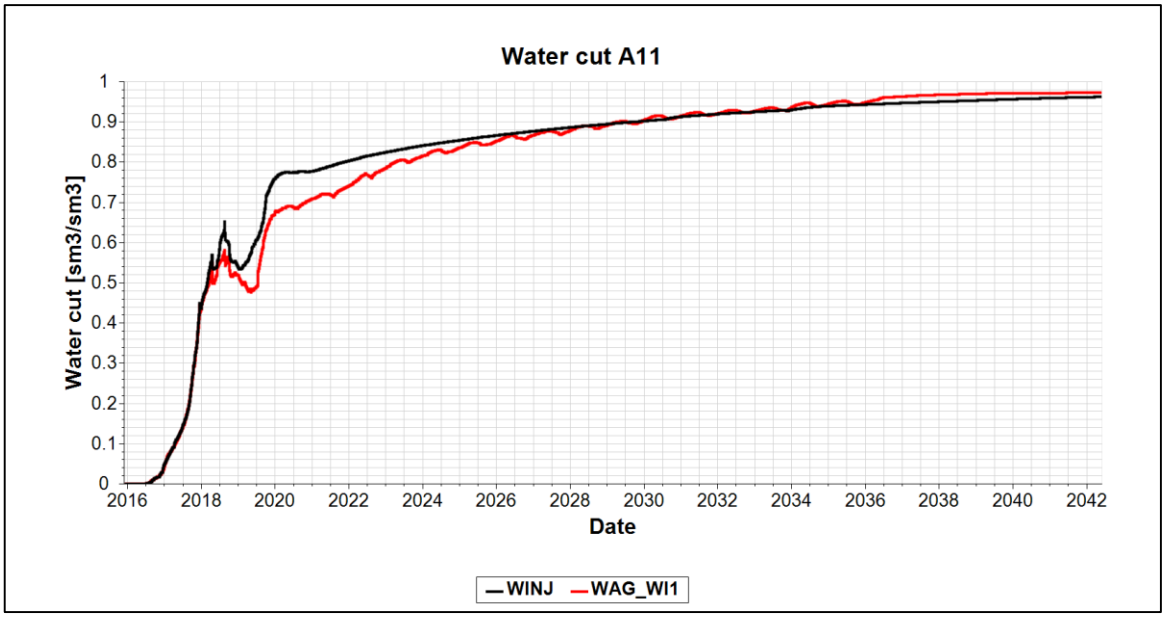

Fig. 4-23 *– Water cut for production well A-11.*

Table 2 *– Recovery results from field simulation for scenario; 1) water injection, 2) WAG with injection of 1 · 10^6 Sm^3/day gas in injector WI1, and 3)) WAG with injection of 1 · 10^6 Sm^3/day gas in injector WI1 and WI3. The gas left in reservoir for scenario 3 is abnormally high because the injector WI3 kept injecting gas until the end by mistake of the author.*

Scenario	Recovery factor	Cumulative oil production [10^6 Sm^3]	Increase oil [%]	Increase in oil equivalents [%]	Gas left in reservoir [10^6 Sm^3]
1	0.489	32,1			
2	0.508	33,3	3,87	3,25	199
3	0.520	34,2	6,47	5,13	429

5 Discussion

Some of the benefits and possible pitfalls regarding WAG injections has been investigated during this paper. As seen in section 4.1.5, it is important that the reservoir exhibit the right characteristics for a successful WAG injection project. Proper input data and choice of models affects simulation results.

5.1 Uncertainty in Relative Permeability

The simulation in this paper is conducted with two-phase relative permeability input data. An interpolation model is used to represent three-phase relative permeability. This is the most common way to deal with three-phase flow. During WAG, the cyclic injection of water and gas into the three-phase region increases the importance of accuracy in the relative permeability. **Fig. 5-1** illustrates the importance of input data in the model.

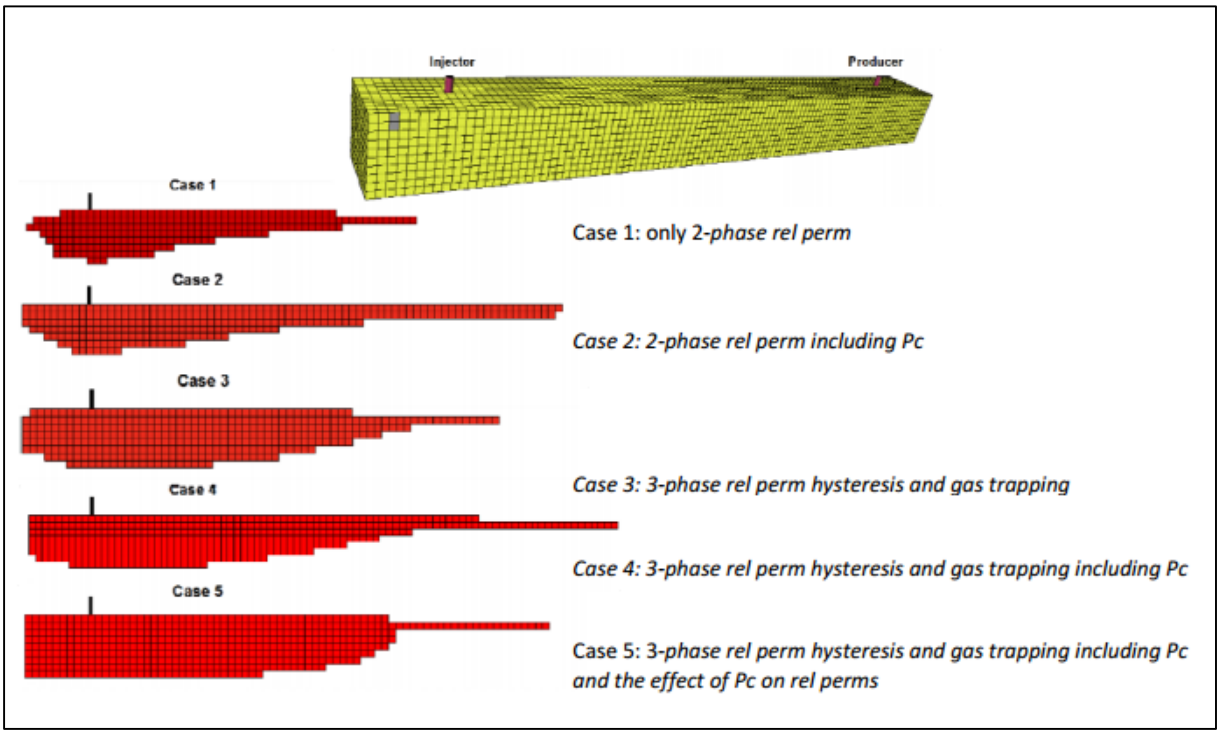

Fig. 5-1 *– Extension of three-phase zone for different input data (Skauge & Sorbie, 2014)*

If it is not possible for some reason to obtain ideal input data (three-phase relative permeability lab results are still very expensive), best solution with the available data should be sought after. (Skauge & Sorbie, 2014) suggest following recommendations for modelling of the different phases based on three-phase WAG flow experiments. The recommendations are supplied with additional information.

1) *Water* relative permeability should vary with water and gas saturation.
   i. The dependency of gas saturation is backed up by results in (Spiteri & Juanes, 2004), which show that the largest errors in water relative permeability arise when water is injected after a gas flood.

2) Residual *oil* should vary with trapped gas saturation and oil relative permeability should be history dependent.
   i. (Spiteri & Juanes, 2004) compares the three common three phase interpolation models for oil relative permeability: Stone I, Stone II and Baker. Results show that Stone I gives best match with three-phase core experiments, while Stone II might underestimate the oil relative permeability significantly.

3) *Gas* relative permeability should vary with gas saturation, water saturation and gas trapping history.
   i. Results in (Spiteri & Juanes, 2004) confirm the importance of gas trapping history for correct estimation of gas relative permeabilities during water injection after gas flood. For this saturation path, two-phase gas relativity is overestimated compared with experimental results.

5.2 Gas Trapping

The effect of gas trapping is quite significant. It reduces the relative permeability of both injected water and gas **Fig. 4-6** and **Fig. A- 8**. This leads to decrease in mobility, which is favorable for optimal displacement of the oil. The gas trapping also increase the connectivity of oil, when displacing it from larger pores. This makes it possible for the water to displace additional oil. The downside of the gas trapping is the gas left in the reservoir after the field is abandoned. This decreases the overall energy output of a WAG injection project.

For simulation purposes, it seems that it is important to include gas-trapping hysteresis. Without this, the proper effect of WAG will not be evident as the gas saturation in the three-phase zone reduces to initial critical saturation between every cycle, thus the relative permeability near the injection well is likely to be overestimated.

5.3 Gas-Oil Ratio

A high gas-oil ratio can be a cause for concern. A platform has an upper limit on how much gas can be processed at a certain time. A high gas-oil ratio may then restrict the oil production, as was the result during WAG injection at the Brage field (Lien et al., 1998). .

In order to restrict the gas-oil ratio, a reduction in injected gas proportional to the decline in oil production could be a strategy. **Fig. 4-4** show how the gas-oil ratio and cumulative oil production is affected by this reduction. The gas-oil ratio for the reduced gas injection case is much more balanced than for the constant gas injection case. Though the oil production is faster for the constant gas injection, the ultimate recovery is about the same.

Active surveillance of the GOR seems to be important during a WAG injection process. If the GOR suddenly starts to increase with a concerning rate, counter measures such as decreasing the gas injection rate or shortening the time of the gas cycle could be possible solutions. As seen in section 4.1.1 and 4.1.2, change in the gas injection rate and gas cycle length affects the GOR much more than the oil production. Keep in mind that these results are without hysteresis.

5.4 Compositional Effects

Compositional effects due to gas injection have been show in section 4.1.6. The interaction between gas and oil leads to compositional changes in both phases; most importantly, it could increase the mobility of the oil. The effect could be tested out further with different compositions of the injection gas, with emphasis on checking if higher ratio of light components could significantly increase the oil recovery. Running a full-scale compositional model that includes gas-trapping hysteresis is a computational demanding task.

5.5 High Permeability Layers

High permeability layers in the top of the formation results in less extension of the gas since it creates a high mobility zone in this layer faster than the other layers. It would on the other hand be ideal to have low permeability layers in the top and higher permeability layers further down in the water region. This way the water and gas would have more even mobility since the viscosity of the gas is much lower than the viscosity of the water.

5.6 WAG Potential in Field Model

Assume, based on the result in **Table 1** that gas-trapping hysteresis causes an increase in additional oil recovery of 30% compared with the non-hysteresis case. Also, assume that incremental increase in oil equivalents in the hysteresis case is half of the incremental increase in oil. Based on the field case results in **Table 2**, this will give an incremental increase in oil recovery of 5% and an incremental oil equivalent recovery of 2.5% for scenario 1. This means that we have a total increase in extracted energy from the field, which is an important criterion for WAG injection.

The additional WAG potential from injection well WI3 is shown to be less than the potential from WI1.

Low permeability and/or initial pressures close to the bubble point can force the pressure below the bubble point. This leads to gas out of solution, which segregates upwards and will eventually form a gas layer in the top of the formation. If WAG injection follows this process, then the gas would likely follow the existing gas layer, due to high gas mobility, thus much of the WAG potential might be lost.

6 Conclusion

- It has been shown through the field model simulation results that WAG injection from injector WI1 has the potential to increase overall energy output of the reservoir by around 2.5 percent assuming simulation results from the simplified model are representative of the field model.
- Gas trapping increases the oil recovery, but result in large amounts of gas left in the reservoir.
- High permeable layers in the top of the reservoir has the potential of reducing the effect of the WAG injection, at least in the beginning of the WAG injection. Unfinished simulation results show that some of the effect of the WAG injection comes later. Rapid increases and deceases in GOR can be expected.
- Due to reduction in water relative permeability around the injection well, water injectivity is likely to be reduced. If water injection from the well in question is critical, it could be wise to established if the well has a buffer when it comes to injectivity.
- Compositional effects resulting from the gas injection has been shown. If the injection-gas contains higher ratio of lighter components the effect is likely to be stronger. The stripping effect can only be handled by compositional simulation. The significance of the compositional effects, and whether or not a black –oil simulator can still be used for WAG injection remains unanswered.
- Gas-oil ratio is a concerning factor during WAG injection and should be under active surveillance. When rapid increases are observed, one should consider counter measures such as decreasing the gas injection rate or decreasing the time of gas injection, of both.

Bibliography

Carlson, F. M. (1981). *Simulation of Relative Permeability Hysteresis to the Nonwetting Phase*. Paper presented at the SPE Annual Technical Conference and Exhibition, San Antonio, Texas.

Choudhary, M. K., Parekh, B., Dezabala, E., Solis, H. A., Pujiyono, P., & De Narvaez, J. Z. Z. (2011). *Design, Implementation and Performance of a Down-Dip WAG Pilot*. Paper presented at the International Petroleum Technology Conference, Bangkok, Thailand.

Christensen, J. R., Larsen, M., & Nicolaisen, H. (2000). *Compositional Simulation of Water-Alternating-Gas Processes*. Paper presented at the SPE Annual Technical Conference and Exhibition, Dallas, Texas.

Christensen, J. R., Stenby, E. H., & Skauge, A. (1998). *Review of WAG Field Experience*. Paper presented at the International Petroleum Conference and Exhibition of Mexico, Villahermosa, Mexico.

Crogh, N. A., Eide, K., & Morterud, S. E. (2002). *WAG Injection at the Statfjord Field, A Success Story*. Paper presented at the European Petroleum Conference, Aberdeen, U.K.

Dake, L. P. (1998). *Fundamentals of Reservoir Engineering* (17th ed.). Amsterdam: Elsevier Science B.V.

Dake, L. P. (2001). *The Practice of Reservoir Engineering* (Revised ed.). Amsterdam: Elsevier Science B.V.

Fai-Yengo, V., Rahnema, H., & Alfi, M. (2014). *Impact of Light component Stripping During CO2 injection in Bakken Formation.* Paper presented at the Unconventional Resources Technology Conference, Denver, Colorado.

Fatemi, S. M., & Sohrabi, M. (2012). *Experimental and Theoretical Investigation of Water/Gas Relative Permeability Hysteresis: Applicable to Water Alternating Gas (WAG) Injection and Gas Storage Processes*. Paper presented at the Abu Dhabi International Petroleum Conference and Exhibition.

Fettke, C. R. (1938). The Bradford Oil Field, Pennsylvania and New York. *Mineral Resources Report M21, Pennsylvania Geological Survey*.

Kamath, J., Nakagawa, F. M., Boyer, R. E., & Edwards, K. A. (1998). *Laboratory Investigation of Injectivity Losses During WAG in West Texas Dolomrites*.

Killough, J. E. (1976). Reservoir Simulation With History Dependent Saturation Functions. *SPE Journal, 16*(1), 12.

Klinkenberg, L. J. (1941). *The Permeability Of Porous Media To Liquids And Gases*. Paper presented at the API Eleventh Mid-Year Meeting, Tulsa (OK).

Kossack, C. A. (2000). *Comparison of Reservoir Simulation Hysteresis Options*. Paper presented at the SPE Annual Technical Conference and Exhibition, Dalla, Texas.

Kumar, M., Senden, T., Knackstedt, M. A., Latham, S. J., Sok, R. M., Sheppard, A. P., . . . Pinczewski, V. L. (2009). Imaging of Pore Scale Distribution of Fluids And Wettability. *Society of Petrophysicists and Well-Log Analysts, 50*(04).

Land, C. S. (1968). Calculation of Imbibition Relative Permeability for Two- and Three-Phase Flow From Rock Properties. *SPE Journal, 8*(2), 8.

Larsen, J. A., & Skauge, A. (1998). Methodology for Numerical Simulation With Cycle-Dependent Relative Permeabilities. *SPE Journal, 3*(2), 11.

Lien, S. C., Lie, S. E., Fjellbirkeland, H., & Larsen, S. V. (1998). *Brage Field, Lessons Learned After 5 Years of Production*. Paper presented at the European Petroleum Conference, The Hauge, Netherlands.

Nolen-Hoeksema, R. (2014). Defining Permeability: Flow Through Pores. *Oilfield Review*(Autumn), 2.

Oak, M. J. (1990). *Three-Phase Relative Permeability of Water-Wet Berea*. Paper presented at the SPE/DOE Enhanced Oil Recovery Symposium, Tulsa, Oklahoma.

Oren, P. E., Bakke, S., & Arntzen, O. J. (1998). Extending Predictive Capabilities to Network Models. *SPE Journal, 3*(04), 13. doi:10.2118/52052-PA

Petrowiki. (2016). Compositional effects during immiscible gas injection. Retrieved from http://petrowiki.org/Compositional_effects_during_immiscible_gas_injection

Sehbi, B. S., Frailey, S. M., & Lawal, A. S. (2001). *Analysis of Factors Affecting Microscopic Displacement Efficiency in CO2 Floods*. Paper presented at the SPE Permian Basin Oil and Gas Recovery Conference, Midland, Texas.

Skauge, A., & Dale, E. I. (2007). *Process in immiscible WAG modeling*. Paper presented at the SPE/EAGE Reservoir Characterization and Simulation Conference, Abu Dhabi, UAE.

Skauge, A., & Sorbie, K. (2014). *Status of Fluid Flow Mechanisms for Miscible and Immiscible WAG*. Paper presented at the SPE EOR Conference at Oil and Gas West Asia, Muscat, Oman.

Spiteri, E. J., & Juanes, R. (2004). *Impact of Relative Permeability Hysteresis on the Numerical Simulation of WAG Injection*. Paper presented at the SPE Annual Technical Conference and Exhibition, Houston, Texas.

Suicmez, V. S., Piri, M., & Blunt, M. J. (2006). *Pore-Scale Modeling of Three-Phase WAG injection: Prediction of relative Permeabilities and Trapping for Different Displacement Cycles*. Paper presented at the SPE/DOE Symposium on Improved Oil Recovery, Tusla, Oklahoma.

Torrey, P. D. (1951). *A Review of Some Important Water-Injection Projects*. Paper presented at the Drilling and Production Practice, New York, New York.

Appendix A Additional Simulation Results

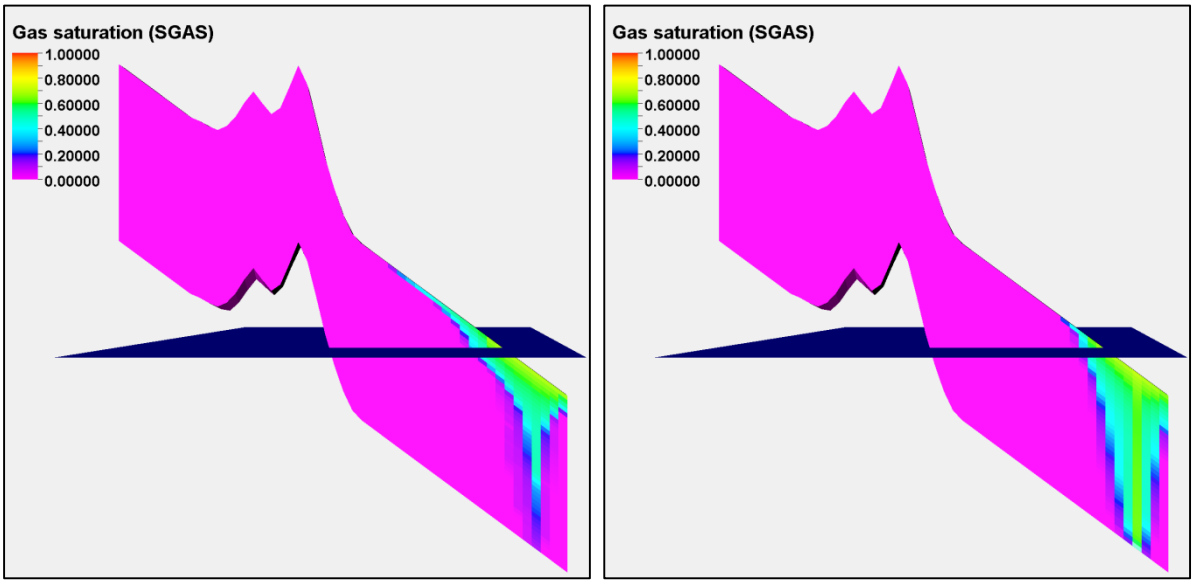

Fig. A- 1 *– Gas saturation, one month after initiation of gas injection , for simulation with (right) and without (left) gas-phase hysteresis. Lands trapping coefficient, C = 1. Date: 28.11.16*

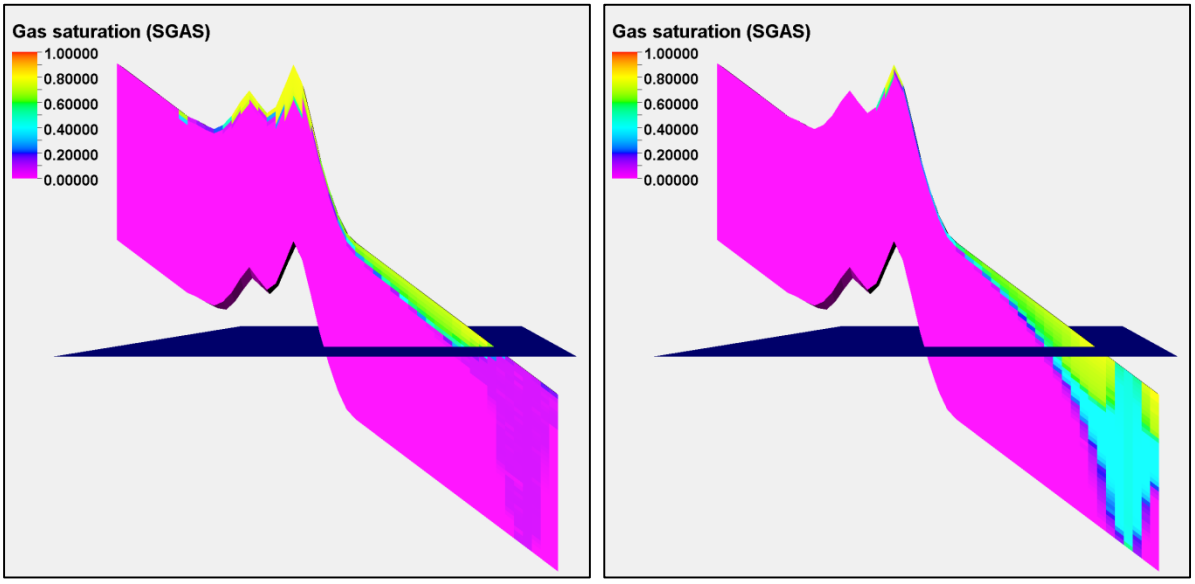

Fig. A- 2 *– Gas saturation, two months after end of first gas cycle , for simulation with (right) and without (left) gas-phase hysteresis. Lands trapping coefficient, C = 1. Date: 28.04.17*

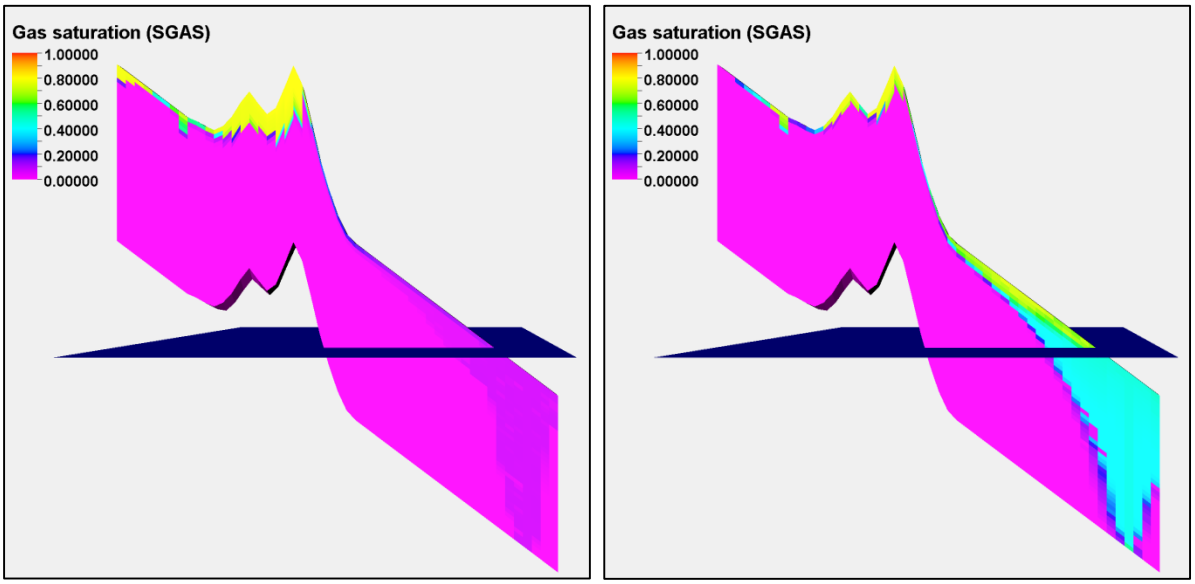

Fig. A- 3 *– Gas saturation, at end of second water cycle, for simulation with (right) and without (left) gas-phase hysteresis. Lands trapping coefficient, C = 1. Date: 28.10.17*

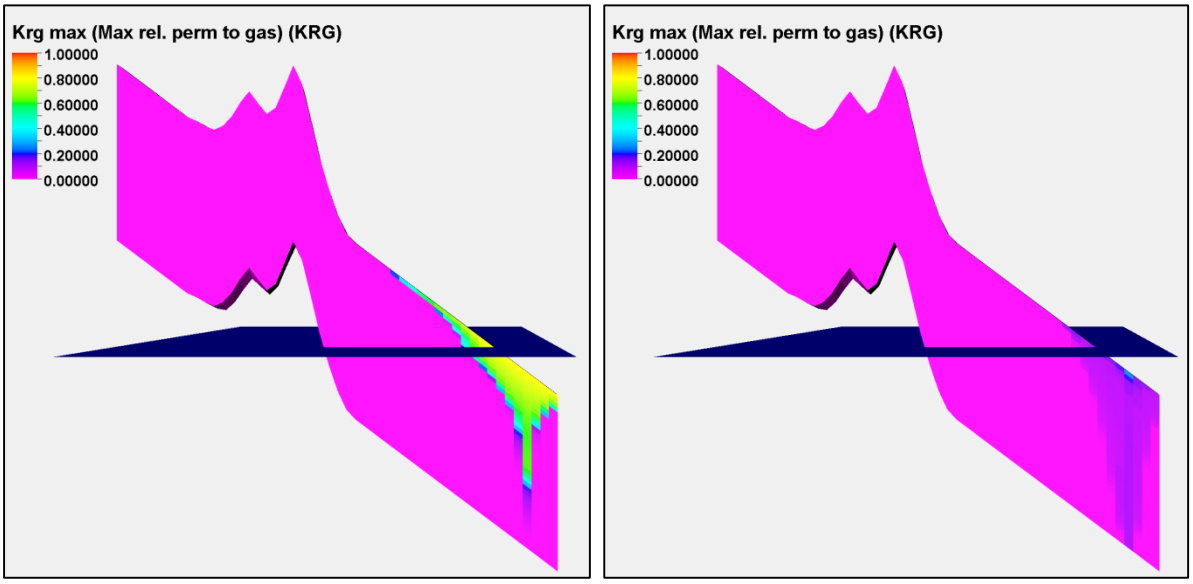

Fig. A- 4 *- Gas relative permeability, one month after initiation of gas injection , for simulation with (right) and without (left) gas-phase hysteresis. Lands trapping coefficient, C = 1. Date: 28.11.16*

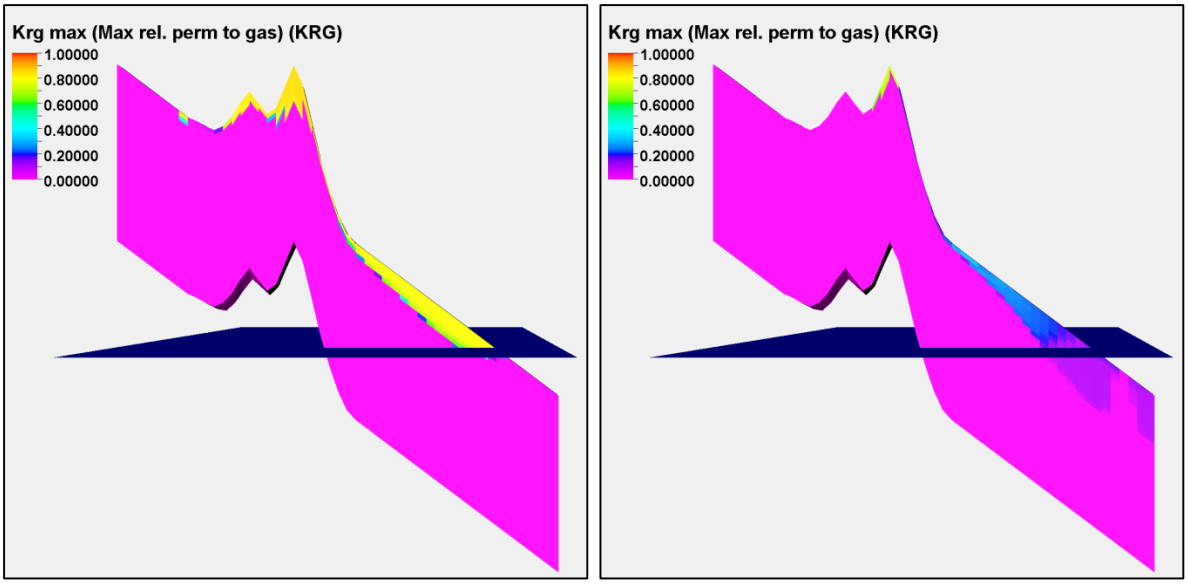

Fig. A- 5 *– Gas relative permeability, two months after end of first gas cycle , for simulation with (right) and without (left) gas-phase hysteresis. Lands trapping coefficient, C = 1. Date: 28.04.17*

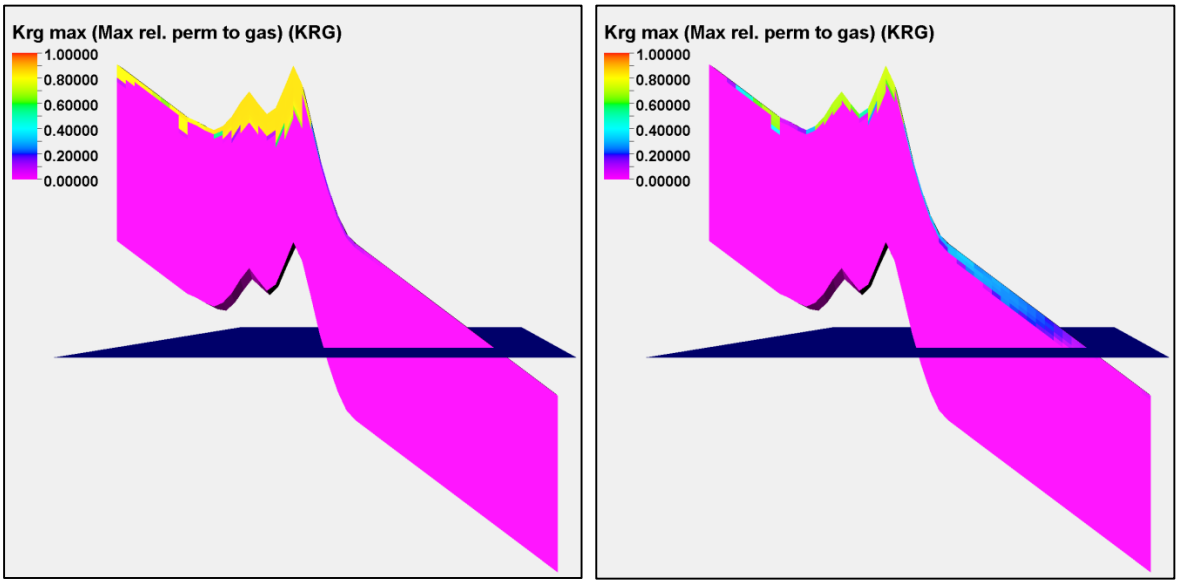

Fig. A- 6 *– Gas relative permeability, at end of second water cycle , for simulation with (right) and without (left) gas-phase hysteresis. Lands trapping coefficient, C = 1. Date: 28.10.17*

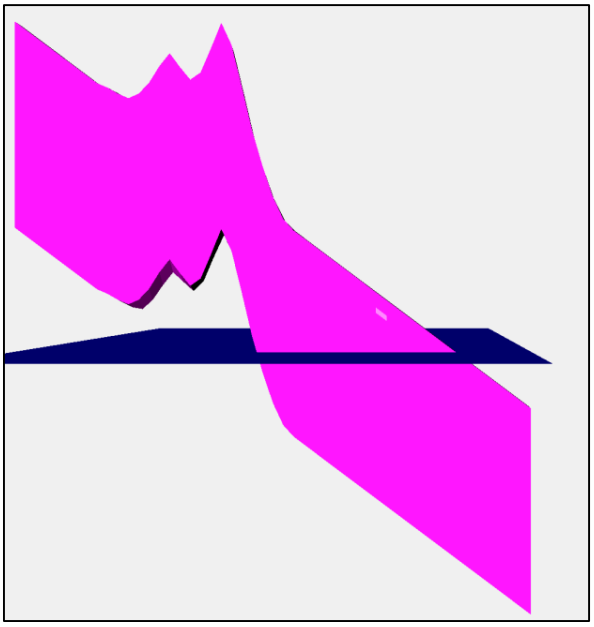

Fig. A- 7 *– Location of grid block (15, 12, 4)*

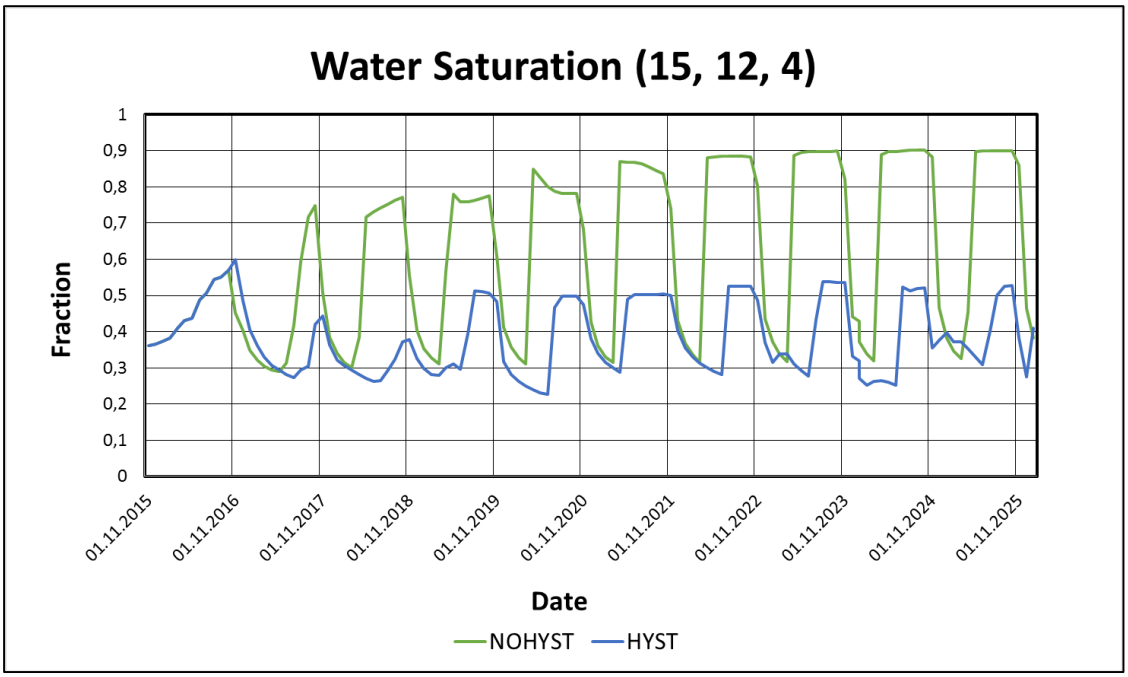

Fig. A- 8 *– Water saturation in grid block (15, 12, 4) for simulation with and without gas-phase hysteresis.*

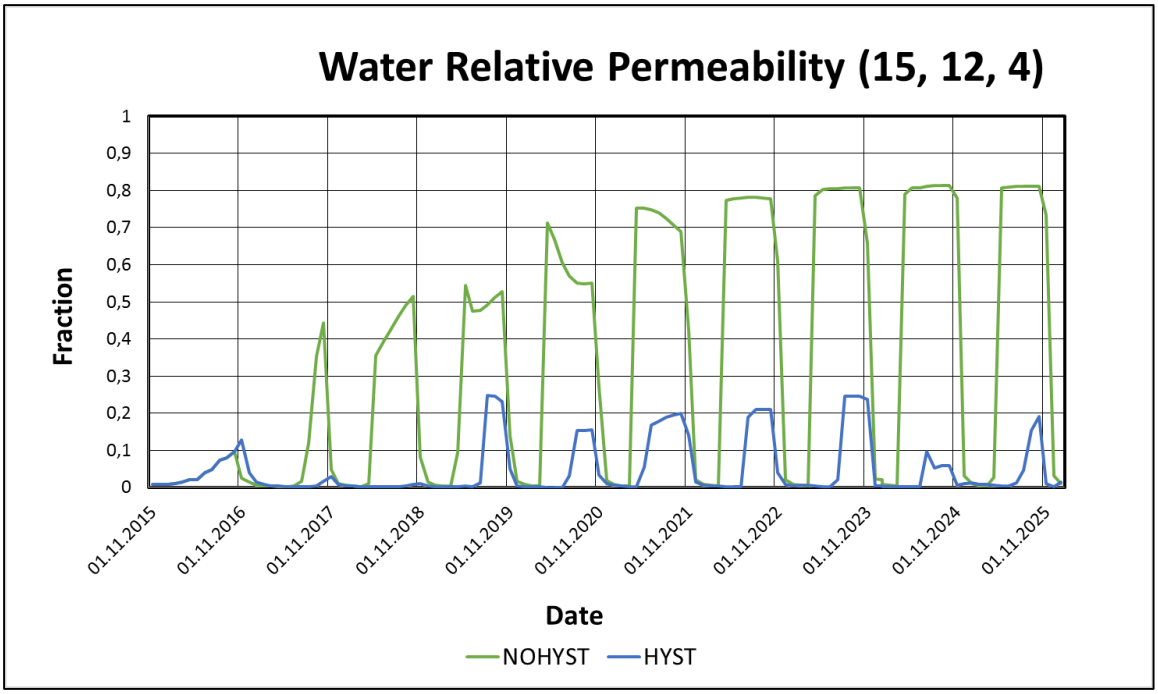

Fig. A- 9 *– Water relative permeability in grid block (15, 12, 4) for simulation with and without gas-phase hysteresis.*

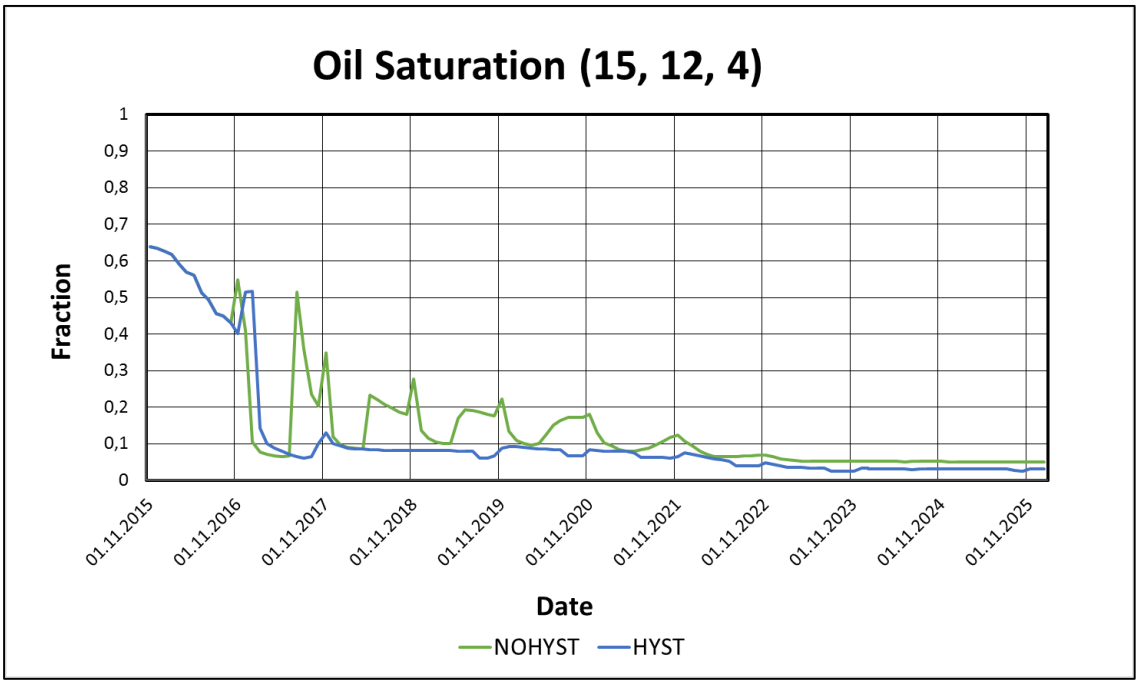

Fig. A- 10 *– Oil saturation in grid block (15, 12, 4) for simulation with and without gas-phase hysteresis.*

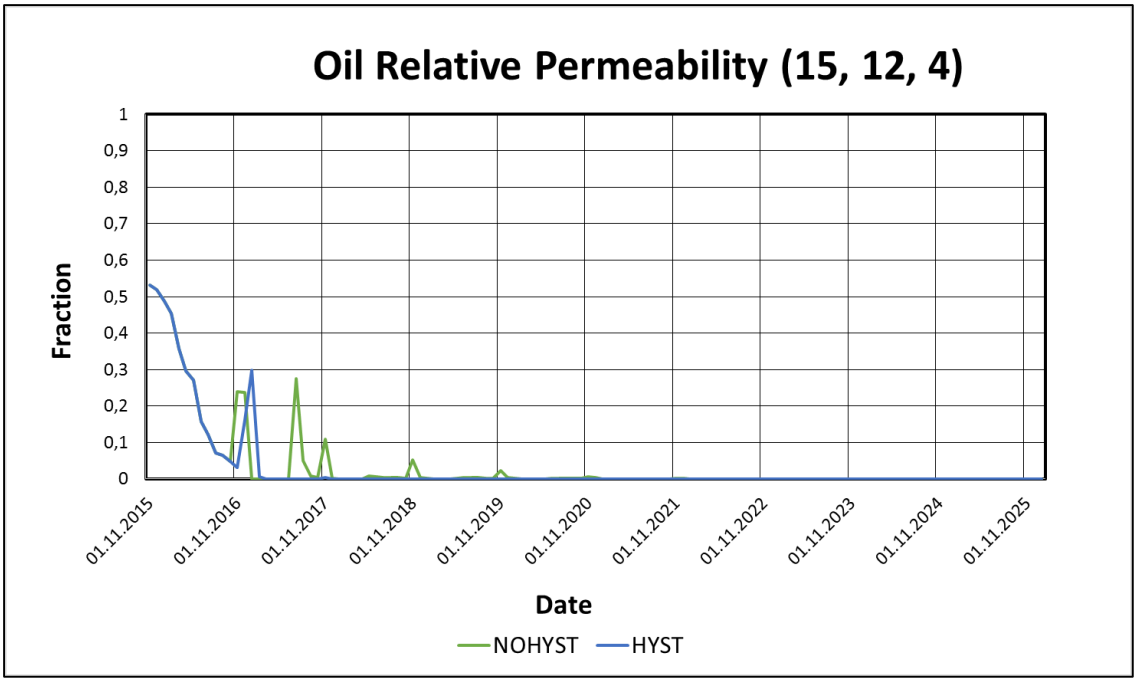

Fig. A- 11 *– Oil relative permeability in grid block (15, 12, 4) for simulation with and without gas-phase hysteresis.*

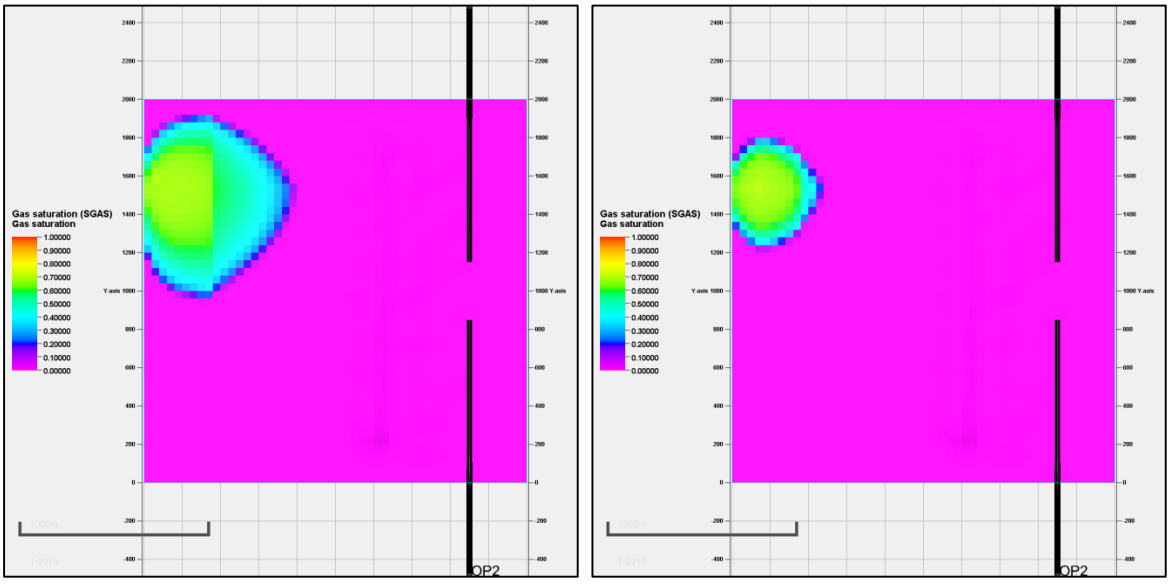

Fig. A- 12 *– 2D gas saturation for case without (left) and with (right) gas trapping hysteresis. One month after gas injection starts.*

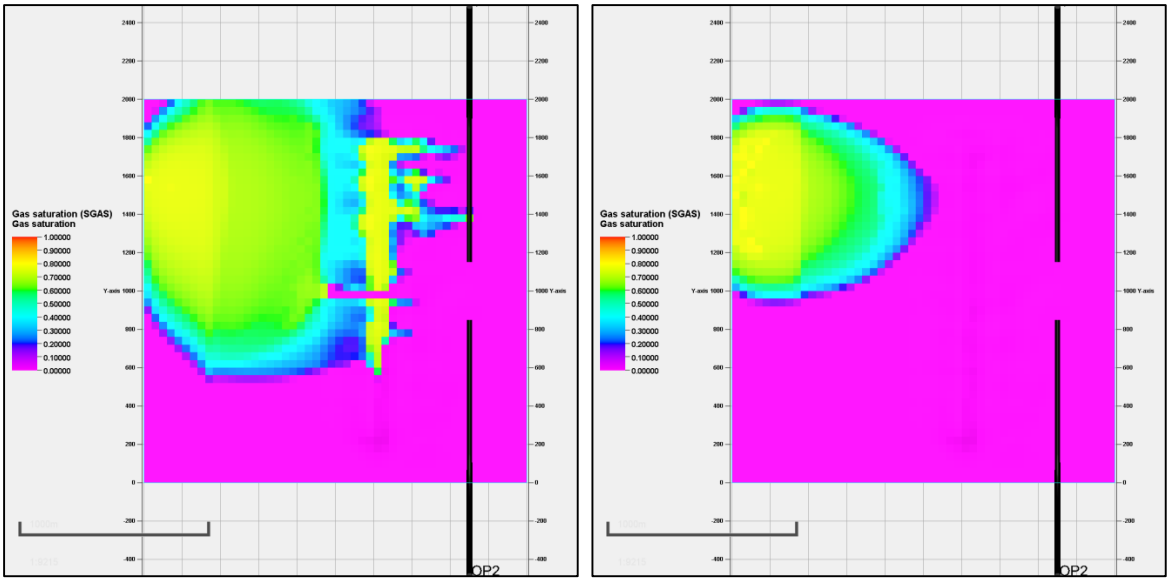

Fig. A- 13 *– 2D gas saturation for case without (left) and with (right) gas trapping hysteresis. At gas breakthrough for the non-hysteresis case.*

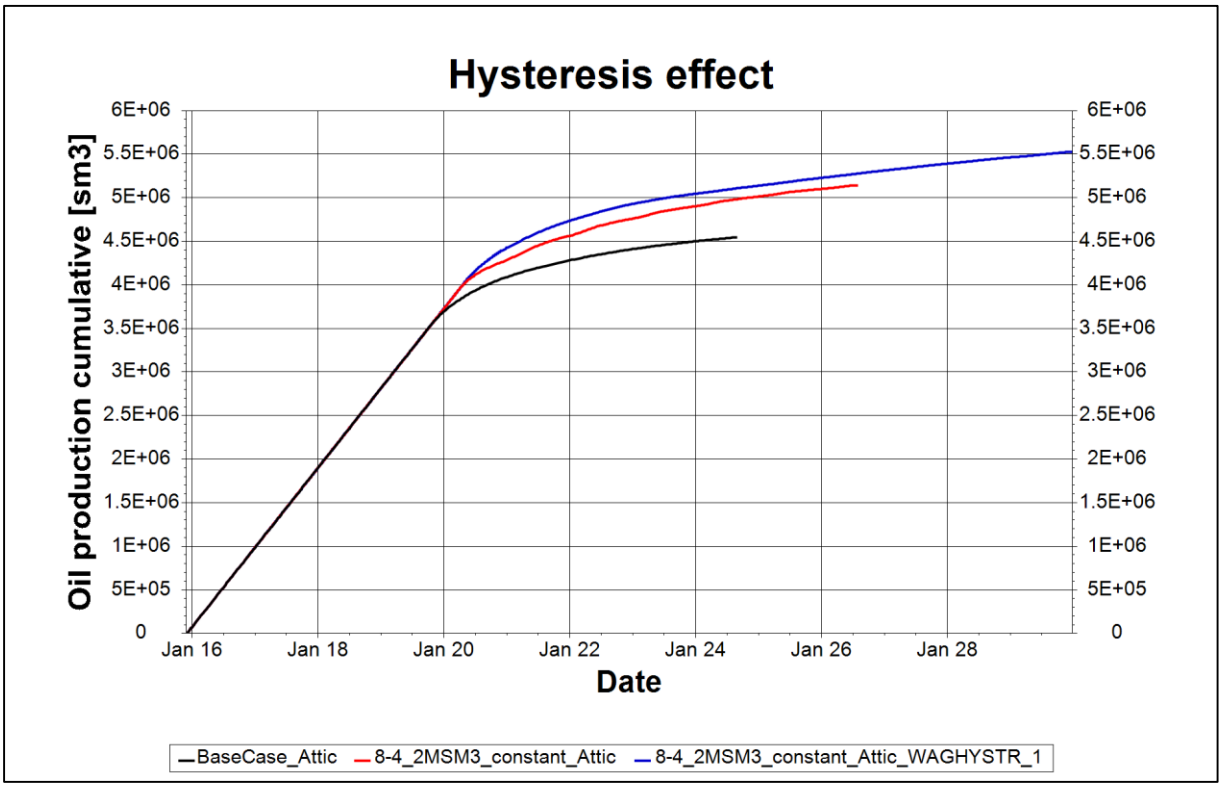

Fig. A- 14 *– Cumulative oil production for base case and WAG with and without hysteresis.*

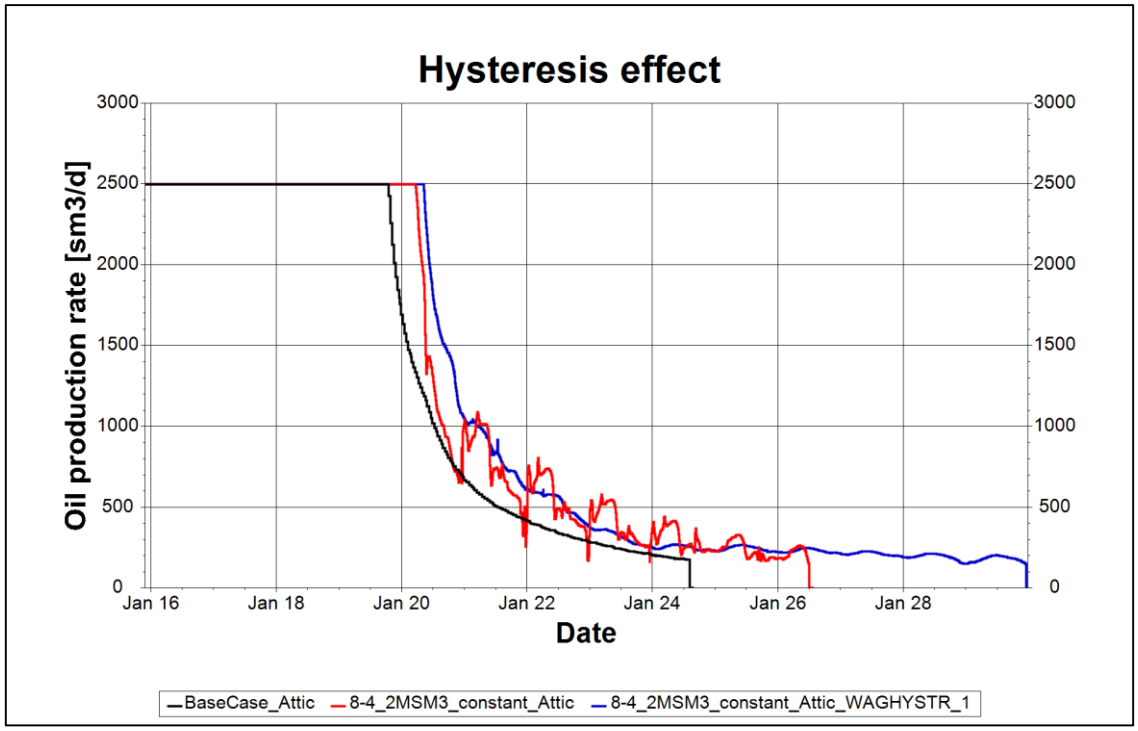

Fig. A- 15 *– Oil production rate for base case and WAG with and without hysteresis.*

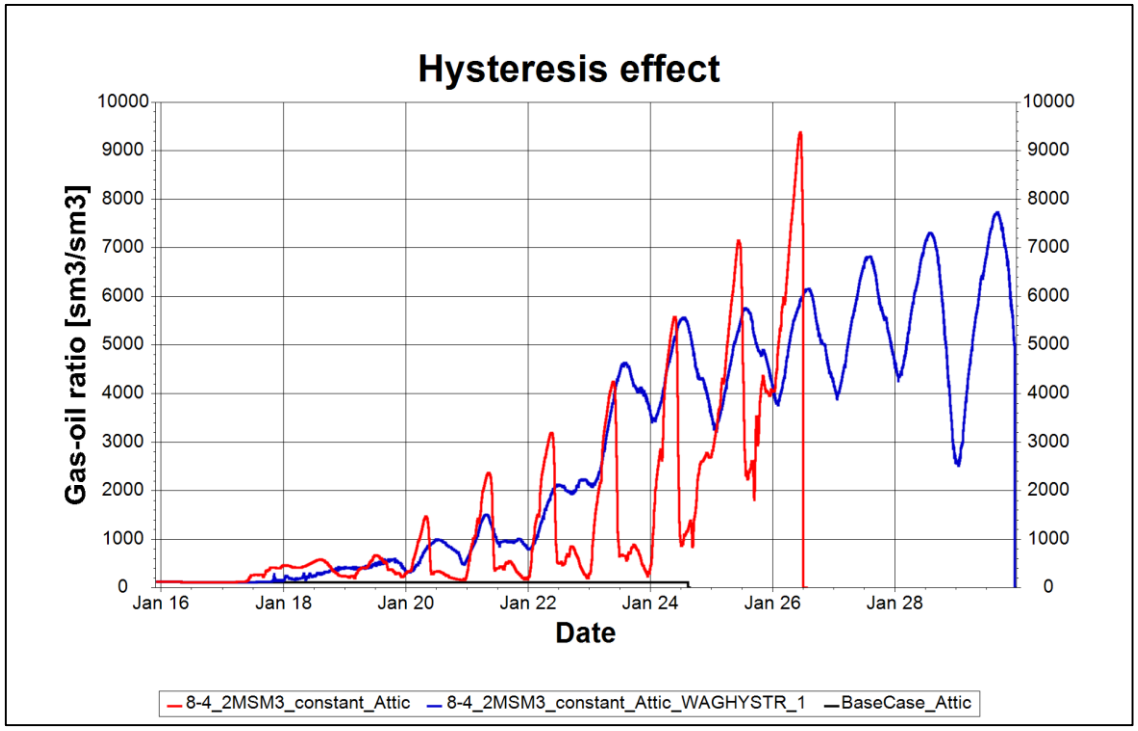

Fig. A- 16 *– GOR for base case and WAG with and without hysteresis.*

Appendix B Reservoir properties, strategy and fluid model for the simplified model.

Table B- 1 *– Reservoir properties and initial conditions for base case in the simplified model*

Reservoir properties	**Description**	**Unit**
Reservoir size (x, y, z)	2000 × 2000 × 40	m
Number of grid blocks	50 × 50 × 40	
Top reservoir	-1875	m
Bottom reservoir	-1990	m
Dip angle	2,15	°
Horizontal permeability	2000	md
Vertical permeability	200	md
Kv/kh	0,1	
Porosity	28 %	
Initial conditions		
Reservoir pressure	194,07	bara
Reservoir temperature	80,9	°C
WOC	-1939	m
STOOIP box model	$13{,}57 \cdot 10^6$	Sm^3
STOOIP attic model	$14{,}70 \cdot 10^6$	Sm^3

Table B- 2 *– Production and injection data for simplified model*

Well start dates	**Description**	**Unit**
OP1 production	28-11-15	
WAG1 injection	28-02-16	
OP2 production	28-05-16	
WAG2 injection	28-08-16	
Targets and limits		
Oil production target per well	2500	Sm^3/day

Liquid production limit per well	5000	Sm^3/day
Water injection upper limit per well	10000	Sm^3/day
Water injection strategy	Group voidage (injecting reservoir volume equals producing reservoir volume)	
Water cut limit	0,97	

Table B- 3 *– Aquifer properties in the simplified model.*

Aquifer properties	**Description**	**Unit**
Numerical aquifer cell 1		
Datum	-1990	m
Permeability	400	md
Cross sectional Area	10’000	m^2
Length	2’000	m
Numerical aquifer cell 2		
Datum	-1990	m
Permeability	200	md
Cross sectional Area	10’000’000	m^2
Length	12’000	m

Table B- 4 *– Reservoir Fluid properties (metric units).*

Comp	MW	T_{crit}	P_{crit}	V_{crit}	Z_{crit}	Vol shift	Acc. factor	Parachor	Ω_a	Ω_b
N2+C1	16,2792	188,412	45,5919	0,09869	0,28721	-0,1938	0,00909	76,067	0,45724	0,0778
CO2+C2	30,2142	305,382	49,2147	0,14719	0,28528	-0,1431	0,09992	108,434	0,45724	0,0778
C3-C4	48,7121	389,584	40,5301	0,22434	0,28069	-0,1039	0,16614	166,353	0,45724	0,0778
C5-C6	77,9424	484,862	31,8966	0,3349	0,26497	-0,0272	0,2661	248,91	0,45724	0,0778
C7-C12	117,991	580,117	25,9123	0,53911	0,28962	0,06757	0,4212	343,49	0,45724	0,0778
C13-C21	227,405	724,913	18,0068	0,97334	0,29078	0,01626	0,76238	605,494	0,45724	0,0778
C22-C35	378,435	873,752	14,9802	1,69477	0,34946	-0,0873	1,1143	936,543	0,45724	0,0778
C36-C80	661,079	1119,66	13,3423	3,326	0,47669	-0,2384	1,08149	1680,16	0,45724	0,0778

Table B- 5 *– Average fraction values based on eight fluid samples.*

Pressure (bar)	160,6
Temperature (°C)	80,9
Elevation (m)	-1923,5
Components	Fraction
N2+C1	34,5
CO2+C2	8,5
C3-C4	13,4
C5-C6	6,4
C7-C12	17,6
C13-C21	9,3
C22-C35	6,4
C36-C80	3,9

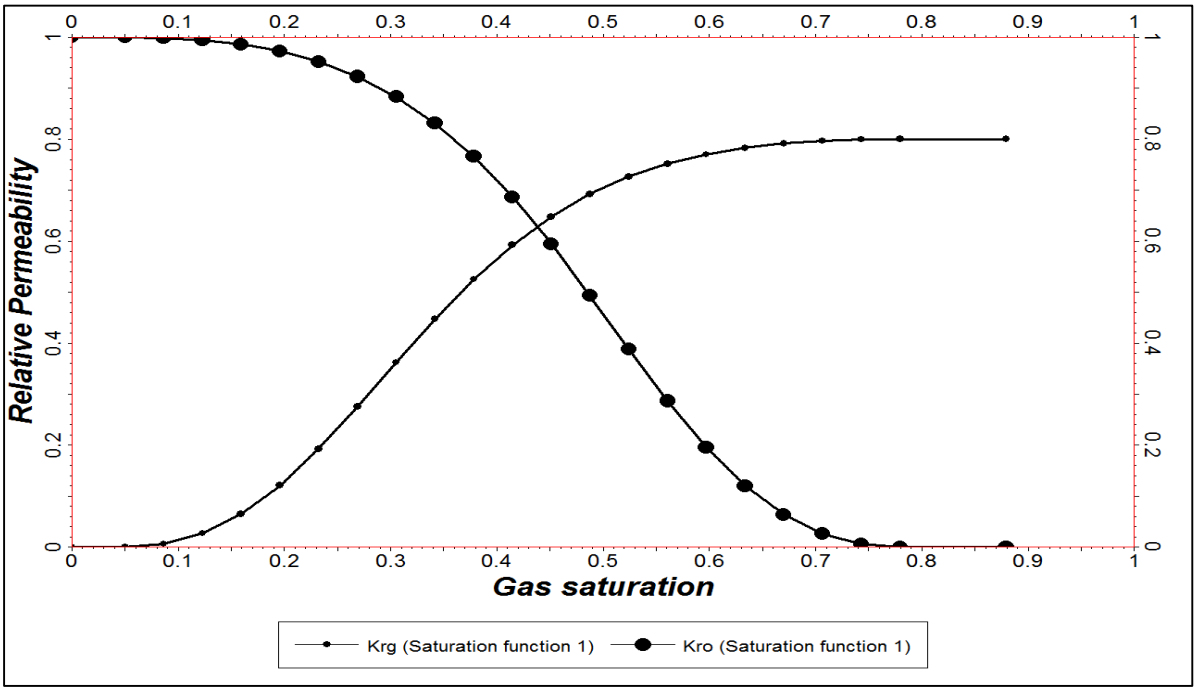

Fig. B- 1 *– Relative permeability curves for two-phase oil and gas system.*

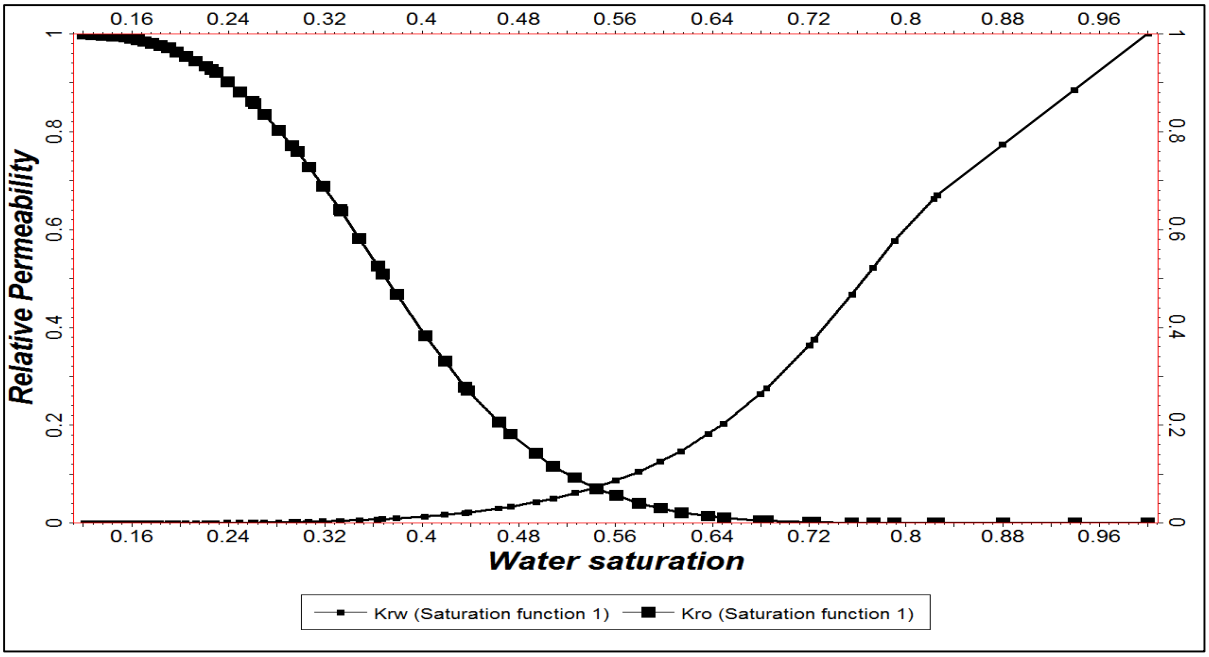

Fig. B- 2 *– Relative permeability curves for two-phase oil and water system.*

Table B- 6 *– Gas-oil saturation function.*

S_g	k_{rg}	k_{rog}	P_{cog}
0	0	1	0
0.05	0	1	0
0.086475	0.006276	0.99874	0
0.12295	0.027232	0.99439	0
0.159425	0.065309	0.98598	0
0.1959	0.12112	0.97225	0
0.232375	0.19263	0.95171	0
0.26885	0.27516	0.92261	0
0.305325	0.36227	0.88306	0
0.3418	0.44737	0.83127	0
0.378275	0.52516	0.76585	0
0.41475	0.59245	0.68648	0
0.451225	0.64803	0.59444	0
0.4877	0.69222	0.49319	0
0.524175	0.72623	0.38832	0

0.56065	0.75164	0.28682	0
0.597125	0.77003	0.19568	0
0.6336	0.78286	0.12038	0
0.670075	0.79137	0.063835	0
0.70655	0.79656	0.02632	0
0.743025	0.79922	0.006029	0
0.7795	0.8	0	0
0.8795	0.8	0	0

Table B- 7 *– Water-oil saturation function.*

S_w	k_{rw}	k_{row}	P_{cow}
0.1205	0	1	2.3444
0.124046	1.01E-06	0.99935	2.1647
0.127714	2.05E-06	0.99867	2.0009
0.131651	3.16E-06	0.99794	1.8463
0.135734	4.32E-06	0.99719	1.7054
0.140004	5.53E-06	0.9964	1.5757
0.144638	6.84E-06	0.99554	1.4521
0.14926	8.15E-06	0.99469	1.3437
0.154474	9.63E-06	0.99373	1.2363
0.155775	1.00E-05	0.99349	1.2128
0.159559	1.99E-05	0.99108	1.1443
0.165276	3.48E-05	0.98745	1.0534
0.170781	4.91E-05	0.98395	0.9764
0.176974	6.53E-05	0.98002	0.9001
0.183452	8.22E-05	0.9759	0.8301
0.190287	0.00010001	0.97156	0.7653
0.19105	0.000102	0.97108	0.75895
0.19739	0.00015538	0.9632	0.7062
0.204586	0.00021597	0.95427	0.6535
0.2128	0.00028513	0.94407	0.6007
0.221102	0.00035502	0.93375	0.554

0.226325	0.000399	0.92727	0.52821
0.22977	0.00046492	0.92044	0.5112
0.239173	0.00064485	0.90179	0.4705
0.249335	0.0008393	0.88164	0.4321
0.259341	0.0010308	0.8618	0.399
0.2616	0.001074	0.85732	0.39242
0.269643	0.0013677	0.83514	0.369
0.281519	0.0018013	0.80238	0.3387
0.292595	0.0022057	0.77183	0.3139
0.296875	0.002362	0.76002	0.30552
0.306437	0.0029624	0.72757	0.2868
0.317962	0.0036861	0.68846	0.267
0.33215	0.004577	0.64031	0.24559
0.333002	0.004663	0.63715	0.2443
0.348172	0.006194	0.58093	0.2244
0.363335	0.0077242	0.52474	0.207
0.367425	0.008137	0.50958	0.20288
0.37911	0.0099456	0.46744	0.1911
0.402373	0.013546	0.38354	0.171
0.4027	0.013597	0.38236	0.17076
0.418772	0.017286	0.33162	0.1588
0.435727	0.021178	0.27808	0.1476
0.437975	0.021694	0.27098	0.14632
0.463522	0.030169	0.20655	0.1318
0.47325	0.033396	0.18202	0.12721
0.494229	0.043251	0.14286	0.1173
0.508525	0.049967	0.11618	0.11169
0.526361	0.061629	0.093056	0.1047
0.5438	0.073031	0.070447	0.099001
0.560326	0.087825	0.056359	0.0936
0.579075	0.10461	0.040376	0.088491
0.597022	0.12623	0.030833	0.0836
0.61435	0.14711	0.021619	0.079668

0.636686	0.18257	0.01463	0.0746
0.649625	0.20311	0.010581	0.072159
0.679627	0.2642	0.0054524	0.0665
0.6849	0.27494	0.004551	0.065671
0.720175	0.36357	0.001594	0.060128
0.724171	0.37527	0.0014568	0.0595
0.75545	0.46689	0.000383	0.055401
0.773009	0.52162	0.00021027	0.0531
0.790725	0.57684	3.60E-05	0.051161
0.823264	0.66277	2.79E-06	0.0476
0.826	0.67	0	0.04735
0.880242	0.77287	0	0.0424
0.93951	0.88528	0	0.0379
1	1	0	0.0337